

Stochastic Interpolants: A Unifying Framework for Flows and Diffusions

Michael S. Albergo^{*1}, Nicholas M. Boffi^{*2}, and Eric Vanden-Eijnden²

¹Center for Cosmology and Particle Physics, New York University

²Courant Institute of Mathematical Sciences, New York University

March 16, 2023

Abstract

We introduce a class of generative models based on the stochastic interpolant framework proposed in [1] that unifies flow-based and diffusion-based methods. We first show how to construct a broad class of continuous-time stochastic processes whose time-dependent probability density function bridges two arbitrary densities exactly in finite time. These ‘stochastic interpolants’ are built by combining data from the two densities with an additional latent variable, and the specific details of the construction can be leveraged to shape the resulting time-dependent density in a flexible way. We then show that the time-dependent density of the stochastic interpolant satisfies a first-order transport equation as well as a family of forward and backward Fokker-Planck equations with tunable diffusion; upon consideration of the time evolution of an individual sample, this viewpoint immediately leads to both deterministic and stochastic generative models based on probability flow equations or stochastic differential equations with a tunable level of noise. The drift coefficients entering these models are time-dependent velocity fields characterized as the unique minimizers of simple quadratic objective functions, one of which is a new objective for the score of the interpolant density. Remarkably, we show that minimization of these quadratic objectives leads to control of the likelihood for generative models built upon stochastic dynamics; by contrast, we show that generative models based upon a deterministic dynamics must, in addition, control the Fisher divergence between the target and the model. Finally, we construct estimators for the likelihood and the cross-entropy of interpolant-based generative models, and demonstrate that such models recover the Schrödinger bridge between the two target densities when explicitly optimizing over the interpolant.

^{*}Authors contributed equally.

Contents

1	Introduction	3
1.1	Background and motivation	3
1.2	Main contributions and organization	4
1.3	Related work	5
1.4	Notations	7
2	Stochastic interpolant framework	7
2.1	Definition and Assumptions	7
2.2	Transport equations, score, and quadratic objectives	10
2.3	Generative models	13
2.4	Likelihood control	14
2.5	Density estimation and cross-entropy calculation	16
3	Design considerations	18
3.1	Spatially linear interpolants	19
3.2	Deterministic vs stochastic generative models	23
3.3	One-sided stochastic interpolants for Gaussian ρ_1	23
3.4	Comparison with score-based diffusion models (SBDM)	26
3.5	Rectifying stochastic interpolants	27
4	Stochastic interpolants and Schrödinger bridges	28
A	Bridging two Gaussian mixture densities	33
B	Proofs	34
B.1	Proof of Theorems 2.6, 2.7, and 2.8, and Corollary 2.9.	34
B.2	Proof of Corollary 2.16	40
B.3	Proofs of Lemmas 2.19 and 2.20, and Theorem 2.21.	41
B.4	Proofs of Lemma 2.23 and Theorem 2.24	44
B.5	Proof of Theorem 3.5	47
B.6	Proof of Lemma 4.2 and Theorem 4.3.	47
C	Experimental Specifications	48

1 Introduction

1.1 Background and motivation

Dynamical approaches for deterministic and stochastic transport have become a central theme in contemporary generative modeling research. At the heart of progress is the idea to apply ordinary or stochastic differential equations (ODE/SDE) to continuously transform samples from a base probability density function (PDF) ρ_0 into samples from a target density ρ_1 (or vice-versa), and the realization that inference over the velocity field in these equations can be formulated as empirical risk minimization over a parametric class of functions [16, 41, 17, 42, 3, 1, 30, 28].

A major milestone was the introduction of score-based diffusion methods (SBDM) [42], which map an arbitrary density into a Gaussian by passing samples through an Ornstein-Uhlenbeck (OU) process. The key insight of SBDM is that this process can be reversed by introducing a backwards SDE whose drift coefficient depends on the score of the time-dependent density of the process. By learning this score – which can be done by minimization of a quadratic objective function known as the denoising loss [48] – the backwards SDE can be used as a generative model that maps Gaussian noise into data from the target. Though theoretically exact, the mapping takes infinite time in both directions, and hence must be truncated in practice.

While diffusion-based methods have become state-of-the-art for tasks such as image generation, there remains considerable interest in developing methods that bridge two *arbitrary* densities (rather than requiring one to be Gaussian), that accomplish the transport *exactly*, and that do so on a *finite* time interval. Moreover, while highest quality results were originally obtained using stochastic sampling techniques for score-based diffusion methods based on SDEs [42], this has been challenged by recent works that find equivalent or better performance with deterministic sampling techniques based on ODEs if the score is learned sufficiently well [22]. If made to match the performance of their stochastic counterparts, ODE-based methods exhibit a number of desirable characteristics that are absent for SDEs, such as an exact, computationally tractable formula for the likelihood and easy application of well-developed adaptive integration schemes for sampling. It is an open question of significant practical importance to understand if there exists a separation in sample quality between generative models based on deterministic dynamics and those based on stochastic dynamics.

In order to satisfy the desirable characteristics outlined in the previous paragraph, here we develop a framework for generative modeling based on the method proposed in [1], with two modifications – one that improves the baseline performance, and one that enables us to quantify explicitly and explore empirically the tradeoffs between stochastic and deterministic models. The approach is built on the notion of a *stochastic interpolant* x_t used to bridge two arbitrary densities ρ_0 and ρ_1 . We will consider more general designs below, but to fix idea the reader can keep in mind:

$$x_t = (1-t)x_0 + tx_1 + \sqrt{2t(1-t)}z, \quad t \in [0, 1], \quad (1.1)$$

where x_0 , x_1 , and z are random variables drawn independently from ρ_0 , ρ_1 , and the standard Gaussian density $\mathcal{N}(0, Id)$, respectively. The stochastic interpolant x_t defined in (1.1) is a continuous-time stochastic process which, by construction, satisfies $x_{t=0} = x_1 \sim \rho_1$ and $x_{t=1} = x_0 \sim \rho_0$. Its paths therefore exactly bridge between samples from ρ_0 at $t = 0$ and from ρ_1 at $t = 1$, without any bias. A key observation is that:

The law of the interpolant x_t at any time $t \in [0, 1]$ can be realized by many different processes, including an ODE and forward and backward SDEs whose drift coefficients can be learned from data.

To see why this is the case, one must consider the probability distribution of the interpolant x_t ; as shown below, for a large class of densities ρ_0 and ρ_1 supported on \mathbb{R}^d , this distribution is absolutely continuous with respect to the Lebesgue measure, and its time-dependent density $\rho(t)$ satisfies a first-order transport equation, as well as forward and backward Fokker-Planck equations in which the

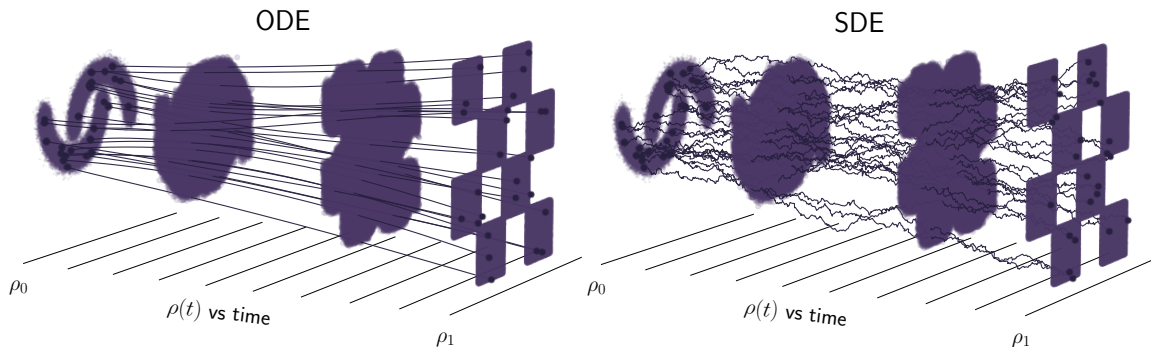


Figure 1: A generative model based on the proposed stochastic interpolant framework connecting two densities with no analytic form. Designing the time-dependent probability density bridging these densities and learning the drift coefficients in its evolution equations is independent of choosing how to sample this density via deterministic or stochastic generative models. *Left panel:* sampling with the probability flow ODE. *Right panel:* Sampling with the SDE with arbitrary noise amplitude, using the same drift as the ODE.

diffusion coefficient can be varied at will. Out of these equations, we can readily derive deterministic and stochastic processes satisfying ODEs and SDEs, respectively, whose densities at time t are given by $\rho(t)$ and hence coincide in law with the original x_t .

Interestingly, the drift coefficients entering these ODE/SDE are the unique minimizers of quadratic objective functions that can be estimated empirically using data from ρ_0 , ρ_1 , and $\mathcal{N}(0, Id)$. The resulting least-squares regression problem allows us to estimate the drift coefficients of the ODE/SDE, which can then be used to push samples from ρ_0 onto new samples from ρ_1 and vice-versa.

1.2 Main contributions and organization

Overall, the approach introduced in this paper is a versatile way to build generative models, with many attractive features that we now summarize.

- Due to the inclusion of the latent variable, the stochastic interpolant defined in Section 2.1 has a probability distribution that is absolutely continuous with respect to the Lebesgue measure, with a density that satisfy a first order transport equation (TE) as well as forward and backward Fokker-Planck equations (FPE) with tunable diffusion coefficients. These equations are given in Section 2.2.
- The drift coefficients entering the TE and the FPE are smoothed spatially by the presence of the latent variable. These coefficients are also the unique minimizers of quadratic objective functions, given in Section 2.2, which are readily amenable to empirical estimation using the available data.
- Due to the inclusion of the latent variable, our approach gives a new loss for the score of the time-dependent PDF of the interpolant, which we give in Section 2.2. This score enters as one component of the drifts in the FPE.
- We can readily derive ordinary differential equations (ODE) as well as forward and backward stochastic differential equations (SDE) associated with the TE and the forward and backward FPE, respectively. These ODE/SDE are given in Section 2.3 and can be used as deterministic or stochastic generative models, with the possibility to again tune their level of diffusivity.

- We show that the approach controls the likelihood of the SDE-based models, generalizing the ScoreFlow approach from score-based diffusion [40]. By contrast, regressing the drift alone is insufficient in general to bound the likelihood with ODE-based models, which require more advanced learning schemes to ensure that the Fisher divergence is also minimized. This is discussed in Section 2.4, where we also show how to optimally tune the level of diffusivity as a function of the error of two components of the drifts.
- We develop a general formula for likelihood evaluation of generative models based on stochastic differential equations that serves as a natural counterpart to the continuous change-of-variables formula that is commonly used to compute the likelihood of a deterministic flow. This is discussed in Section 2.5, where we also show how to estimate the cross-entropy.
- The flexibility of design of the stochastic interpolant is highlighted in Section 3, where we show how the latent variable can be adapted to various tasks (Section 3.1) and how the diffusivity can be tuned for better accuracy (Section 3.2), confirming the picture from the likelihood bounds derived earlier.
- Stochastic interpolants admit a simplified, one-sided version in the special case when ρ_1 is a Gaussian density. This is discussed in Section 3.3, and these one-sided stochastic interpolants allows us to compare our approach with score-based diffusion models (SBDM) in Section 3.4.
- Our approach is amenable to a bias-free variant of the rectification procedure proposed in [30], as discussed in Section 3.5.
- Our approach solves the Schrödinger bridge problem between two densities when maximizing the loss over the interpolant, as discussed in Section 4.
- We highlight the performance of the method on synthetic examples throughout the paper, in particular using Gaussian mixture models for which the drifts are available analytically (as shown in Appendix A).

The above list of features and contributions shows that the proposed method conveniently houses many modeling goals under one roof: it forms a connection between arbitrary densities (allowing for the incorporation of prior knowledge and to directly perform data-to-data translation), reaches the target density on a finite time interval, is versatile in the way it can be adapted to various tasks by exploiting the inherent flexibility in the choice of interpolant, and remains bias-free for any choice of the latent variable amplitude and the noise strength, which can both be tuned as model hyperparameter after training. The method therefore allows us to theoretically and empirically explore the best design choices for learnable diffusive processes, as well as the resulting trade-off between ODE and SDE methods for generative models.

1.3 Related work

Deterministic Transport and Normalizing Flows. Transport-based sampling and density estimation has its contemporary roots in Gaussianizing data via maximum entropy methods [15, 8, 45, 44]. The change of measure under such transformation is the backbone of normalizing flow models. The first neural network realizations of these methods arose through imposing clever structure on the transformation to make the change of measure tractable in discrete, sequential steps [38, 11, 36, 20, 13]. A continuous time version of this procedure was made possible by viewing the map $T = X_t(x)$ as the solution of an ODE [7, 16], whose parametric drift defining the transport is learned via maximum likelihood. Training this way is intractable at scale, as it requires simulating the ODE. As such, various methods introduced regularization on the path taken between the two densities to make the ODE solves more efficient [14, 34, 46], though the inherent obstacle still remains. We also work in the continuous time setting; however, our approach allows for the learning the drift without needing to simulate the dynamics, and can additionally handle diffusive processes.

Stochastic Transport and Score-Based Diffusions (SBDMs). Recent works complementary to the deterministic map approach have realized that connecting a data distribution to a Gaussian density can be viewed as the evolution of an Ornstein-Uhlenbeck (OU) process which gradually degrades samples from the distribution of interest to Gaussian noise [39, 17, 41, 42]. The OU process endows a specific path in the space of probability density functions, and its reverse process likewise creates a path that is dependent on the score of the time-dependent density, $\nabla \log \rho(t)$. The fixed path and ability to sample $\rho(t)$ means that optimization to learn the backward drift amounts to a least-square regression problem under the score-matching framework [21]. Once the score is learned, sampling from the target amounts to evolving the reverse diffusions according to its backward SDE. Moreover, the dynamics of these stochastic processes also emit a probability flow equation at the level of the distribution, first noted [2, 35, 23] and then applied in [32, 40, 24, 4]. This probability flow is used for density estimation and cross-entropy calculations, even though the quantities calculated this are not readily connected to those associated with the SDE. The SDE framework, as it has been originally presented, introduces a number of complexities which are not *a priori* well motivated, including the dependence on mapping to a normal density and the complicated tuning of the time parameterization and noise scheduling [49, 18] as well as the underlying stochastic dynamics [12, 22]. While related efforts have also tried to remove the dependency on the OU backbone of SBDMs [37], these procedures can be overly complicated, relying on inexact mixtures of diffusions with limited expressivity and no accessible probability flow formulation. Our method avoids these complexities by observing that the key idea behind SBDMs, namely the bridging of densities via a time-dependent PDF whose evolution equations is available, can be straightforwardly generalized to a much wider class of processes. This allows us to simplify the picture, working on a finite interval exactly between arbitrary densities.

Stochastic Interpolants, Rectified Flows, and Flow matching. Variants of the stochastic interpolant method presented in [1] were also presented in [30, 28]. In [30], a linear interpolant was proposed with a focus on straight paths. This was employed as a step toward rectifying the transport paths [29] through a procedure which improves sampling efficiency, but introduces a bias. Here, in Section 3.5, we present an alternative form of the rectification that is bias-free. In [28], the interpolant picture was assembled from the perspective of conditional probability paths connecting to a Gaussian, where a noise convolution was used to improve the learning, at the cost of biasing the method. In the method proposed here, we introduce an unbiased means for incorporating noise into the process, both via the introduction of a latent variable into the stochastic interpolant and the inclusion of a tunable diffusion coefficient in the associated stochastic generative models. We also provide theoretical and practical motivation for the presence of these noises.

Optimal Transport and Schrödinger Bridges. There is both theoretical and practical interest in minimizing the transport cost of connecting ρ_0 and ρ_1 , which, in the case of deterministic maps, is characterized by the optimal transport problem and, in the case of diffusive maps, by the Schrödinger Bridge problem [47, 10]. Optimal transport perspectives in flow-based methods have primarily been employed as a regularization penalty [51, 34, 14, 46] or via imposing structure on the parameterization itself [19, 50]. A variety of recent works have formulated the Schrödinger problem in the context of a learnable diffusion [5, 43]. In the interpolant framework, [1, 30, 28] all propose optimal transport extensions to the learning procedure. The method of [30, 29] allows one to sequentially lower the transport cost through rectification, at the cost of introducing a bias unless the velocity field is perfectly learned. The method of [1] proposes an unbiased framework at the cost of solving an additional optimization problem of the interpolant function. The statement of optimal transport in [28] only applies to Gaussians, but is shown to be practically useful in experimental demonstrations.

In the method proposed below, we provide two approaches for optimizing the transport under stochastic dynamics. Our primary approach, based on that of [1], is presented in Section 4. It offers

an alternative route to solving Benamou-Bernier’s hydrodynamic formulation of the Schrödinger bridge problem via maximization of the loss over the interpolant. We stress however that this additional optimization step is not necessary in practice, as our approach leads to bias-free generative models no matter what, albeit not necessarily optimal ones in the OT or Schrödinger bridge sense. Additionally, in Section 3.5 we present a unbiased variant of the recitfication scheme proposed in [30].

Convergence bounds. Inspired by the successes of score-based diffusion, significant recent research effort has been expended to understand the control that can be obtained on suitable distances between the distribution of the generative model and the target data distribution, such as KL, W_2 , or TV. Perhaps the first line of work in this direction is [40], which showed that standard score-based diffusion training techniques bound the likelihood of the resulting SDE model. Importantly, as we show here, the likelihood of the corresponding probability flow is not bounded in general by this technique, as first highlighted in the context of SBDM by [31]. Control for SBDM-based techniques was later quantified more rigorously under the assumption of functional inequalities in a discretized setting by [25], which were removed by [26] and [9] via Girsanov-based techniques. Most relevant to the PDE-based methods considered here is [6], who apply similar techniques in the SBDM context to obtain sharp guarantees with minimal assumptions.

1.4 Notations

Thorough we denote probability density functions as $\rho_0(x)$, $\rho_1(x)$, $\rho(t, x)$, with $t \in [0, 1]$ and $x \in \mathbb{R}^d$, omitting the function arguments when this leads to no confusion. We proceed similarly for other functions of time and space, such as $b(t, x)$ or $I(t, x_0, x_1)$. We use the subscript t to denote the time-dependency of stochastic processes, like e.g. the stochastic interpolant x_t or the Wiener process W_t . To specify that the random variable x_0 is drawn for the probability distribution with density ρ_0 , say, with a slight abuse of notations we use $x_0 \sim \rho_0$. Similarly, we use $N(0, Id)$ to denote both the density and the distribution of the Gaussian random variable with mean zero and covariance identity. We denote expectation by \mathbb{E} , and usually specify what are the random variables this expectation is taken over. With a slight abuse of terminology, we say that the law of the process x_t is $\rho(t)$ if $\rho(t)$ is the density of the probability distribution of x_t at time t .

We use standard notations for function spaces, e.g. $C^1([0, 1])$ is the space of continuously differentiable functions from $[0, 1]$ to \mathbb{R} , $(C^2([0, 1]))^d$ the space of twice continuously differentiable functions from \mathbb{R}^d to \mathbb{R}^d , and $C_0^\infty(\mathbb{R}^d)$ the space of compactly supported, infinitely differentiable function from \mathbb{R}^d to \mathbb{R} . Given a function $b : [0, 1] \times \mathbb{R}^d \rightarrow \mathbb{R}^d$ with value $b(t, x)$ at (t, x) , we use e.g. $b \in C^1([0, 1]; (C^2(\mathbb{R}^d))^d)$ to indicate that b is continuously differentiable in t for all $(t, x) \in [0, 1] \times \mathbb{R}^d$, and that $b(t, \cdot)$ is an element of $(C^2(\mathbb{R}^d))^d$ for all $t \in [0, 1]$.

2 Stochastic interpolant framework

2.1 Definition and Assumptions

We begin by defining the stochastic processes that are central to our approach:

Definition 2.1 (Stochastic interpolant). *Given two probability density functions $\rho_0, \rho_1 : \mathbb{R}^d \rightarrow \mathbb{R}_{\geq 0}$, a stochastic interpolant between ρ_0 and ρ_1 is a stochastic process x_t defined as*

$$x_t = I(t, x_0, x_1) + \gamma(t)z, \quad t \in [0, 1], \quad (2.1)$$

where:

1. $I \in C^2([0, 1], (C^2(\mathbb{R}^d \times \mathbb{R}^d))^d)$ satisfies the boundary conditions $I(0, x_0, x_1) = x_0$ and $I(1, x_0, x_1) = x_1$, as well as

$$\exists C_1 < \infty : |\partial_t I(t, x_0, x_1)| \leq C_1 |x_0 - x_1| \quad \forall (t, x_0, x_1) \in [0, 1] \times \mathbb{R}^d \times \mathbb{R}^d. \quad (2.2)$$

2. x_0, x_1 , and z are random variables drawn independently from ρ_0, ρ_1 , and $\mathbf{N}(0, Id)$, respectively;
3. $\gamma : [0, 1] \rightarrow \mathbb{R}$ satisfies: $\gamma(0) = \gamma(1) = 0$; $\gamma(t) > 0$ for all $t \in (0, 1)$; $\gamma \in C^2((0, 1))$; and $\gamma^2 \in C^1([0, 1])$

Eq. (2.2) requires that $I(t, x_0, x_1)$ does not move too fast along the way from x_0 at $t = 0$ to x_1 at $t = 1$, and as a result does not wander too far from either of these endpoints – this assumption is made for convenience and is not necessary for most arguments below. Later, we will find it useful to consider choices for I that are spatially nonlinear, which we show can recover the solution to the Schrödinger bridge problem. Nevertheless, a simple example that serves as a valid I in the sense of Definition 2.1 is given in (1.1). In Section 3 we discuss how to design the stochastic interpolant in (2.1) and give some of the properties of the corresponding process x_t . Examples of stochastic interpolants are also shown in Figure 2 for various choices of I and γ in (2.1).

Remark 2.2 (Comparison with [1]). The difference between the stochastic interpolant defined in (2.1) and the one originally introduced in [1] is the inclusion of the latent variable $\gamma(t)z$. The objective of the present paper is to elucidate the advantages that this additional term provides. We note that we could generalize the construction by making $\gamma(t)$ a tensor; here we focus on the scalar case for simplicity.

The stochastic interpolant x_t in (2.1) is a continuous-time stochastic process whose realizations are samples from ρ_0 at time $t = 0$ and from ρ_1 at time $t = 1$ by construction. As a result, it offers a way to bridge ρ_0 and ρ_1 – we are interested in characterizing the law of x_t over the full interval $[0, 1]$, as it will allow us to design generative models. Mathematically, we want to characterize the properties of the time-dependent probability distribution $\mu(t, dx)$ such that

$$\forall t \in [0, 1] : \int_{\mathbb{R}^d} \phi(x) \mu(t, dx) = \mathbb{E} \phi(x_t) \quad \text{for any test function } \phi \in C_0^\infty(\mathbb{R}^d). \quad (2.3)$$

where x_t is defined in (2.1) and the expectation is taken independently over $x_0 \sim \rho_0, x_1 \sim \rho_1$, and $z \sim \mathbf{N}(0, Id)$. To this end, we will need to use conditional expectations over x_t ¹, as described in the following definition.

Definition 2.3. Given any $f \in C_0^\infty([0, 1] \times \mathbb{R}^d \times \mathbb{R}^d \times \mathbb{R}^d)$, its conditional expectation $\mathbb{E}(f(t, x_0, x_1, z) | x_t = x)$ is the function of x such that

$$\int_{\mathbb{R}^d} \mathbb{E}(f(t, x_0, x_1, z) | x_t = x) \mu(t, dx) = \mathbb{E} f(t, x_0, x_1, z) \quad (2.4)$$

where $\mu(t, dx)$ is the time-dependent distribution of x_t defined by (2.3), and the expectation on the right-hand side is taken independently over $x_0 \sim \rho_0, x_1 \sim \rho_1$, and $z \sim \mathbf{N}(0, Id)$.

Vector-valued functions have conditional expectations that are defined analogously.

¹Formally, in terms of the Dirac delta distribution, we can write

$$\mathbb{E}(f(t, x_0, x_1, z) | x_t = x) = \frac{\mathbb{E}(f(t, x_0, x_1, z) \delta(x - x_t))}{\mathbb{E} \delta(x - x_t)}$$

and in this notation we also have $\rho(t, x) = \mathbb{E} \delta(x - x_t)$.

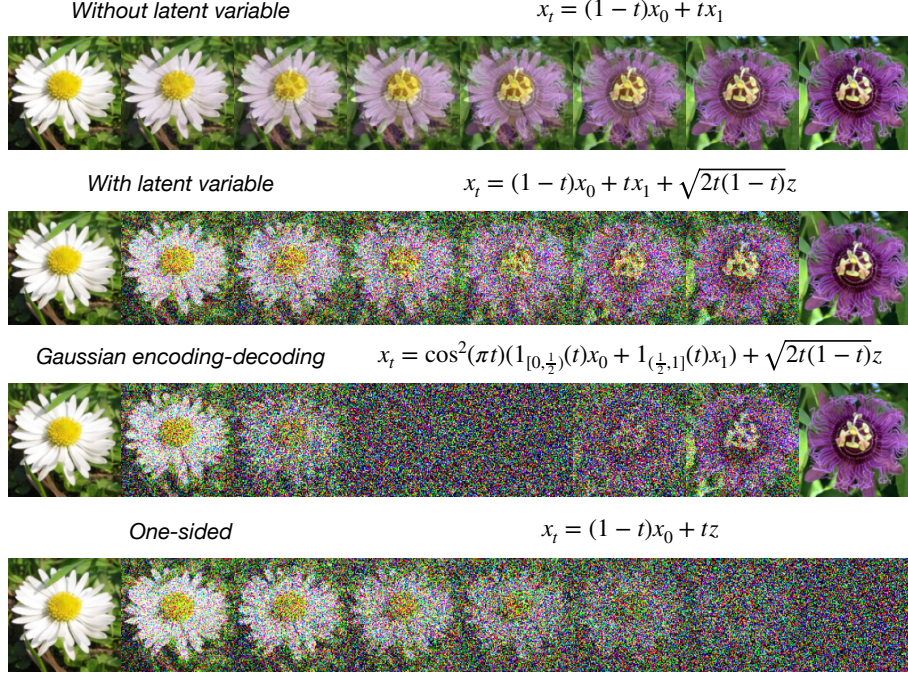


Figure 2: A illustration of the flexibility of designing stochastic interpolants geared toward one’s aims. All examples show one realization of x_t with one $x_0 \sim \rho_0$, and one $x_1 \sim \rho_1$ (the flowers at the left and right of the figures) and one $z \sim \mathcal{N}(0, Id)$. *Top*: interpolating with no latent variable, which reduces to the method of [1]. *Upper middle*: interpolating with the latent variable included, giving a straightforward way of performing image-to-image translation with diffusive processes. *Lower middle*: interpolating with Gaussian encoding-decoding, i.e. turning the signal into noise at mid-point. *Bottom*: one-sided interpolant which reduces to the Gaussian latent variable, with connections to score-based diffusion models.

Remark 2.4. Another seemingly more general way to define the stochastic interpolant is via

$$x'_t = I(t, x_0, x_1) + N_t \quad (2.5)$$

where $N : [0, 1] \rightarrow \mathbb{R}^d$ is a zero-mean Gaussian stochastic process constrained to satisfy $N_{t=0} = N_{t=1} = 0$. As we will show below, our construction only depends on the single-time properties of N_t , which are completely specified by $\mathbb{E}[Z_t Z_t^\top]$. That is, if we take $\gamma(t)$ in (2.1) such that $\mathbb{E}[N_t N_t^\top] = \gamma^2(t) Id$, then the probability distribution of x_t will coincide with that of x'_t defined in (2.5), $x_t \stackrel{d}{=} x'_t$, which is all that matters in our construction. For example, taking $\gamma(t) = \sqrt{t(1 - t)}$ in (2.1) – a choice we will consider below – is equivalent to choosing N_t to be a Brownian bridge in (2.5), i.e. the stochastic process realizable in terms of the Wiener process W_t as $N_t = W_t - tW_1$. This observation will also help us draw an analogy between our approach and the construction used in score-based diffusion models. As we will show below, it is simpler for both analysis and practical implementation to work with the definition (2.1) for x_t .

To proceed, we will also make the following assumption on the PDFs ρ_0, ρ_1 , and their relation to the function I :

Assumption 2.5. *The densities ρ_0 and ρ_1 are strictly positive elements of $C^2(\mathbb{R}^d)$ and are such that*

$$\int_{\mathbb{R}^d} |\nabla \log \rho_0(x)|^2 \rho_0(x) dx < \infty \quad \text{and} \quad \int_{\mathbb{R}^d} |\nabla \log \rho_1(x)|^2 \rho_1(x) dx < \infty. \quad (2.6)$$

The function I satisfies

$$\exists M_1, M_2 < \infty \quad : \quad \mathbb{E}[|\partial_t I(t, x_0, x_1)|^4] \leq M_1; \quad \mathbb{E}[|\partial_t^2 I(t, x_0, x_1)|^2] \leq M_2, \quad \forall t \in [0, 1], \quad (2.7)$$

where the expectation is taken independently over $x_0 \sim \rho_0$ and $x_1 \sim \rho_1$.

Note that for the interpolant (1.1), Assumption 2.5 holds if ρ_0 and ρ_1 both have finite fourth moments.

2.2 Transport equations, score, and quadratic objectives

We now state a result that specifies some important properties of the probability distribution of the stochastic interpolant x_t :

Theorem 2.6 (Stochastic interpolant properties). *The probability distribution of the stochastic interpolant x_t defined in (2.1) is absolutely continuous with respect to the Lebesgue measure at all times $t \in [0, 1]$ and has a time-dependent probability density function (PDF) $\rho(t)$ that satisfies $\rho(0) = \rho_0$, $\rho(1) = \rho_1$, $\rho \in C^1([0, 1]; C^p(\mathbb{R}^d))$ for any $p \in \mathbb{N}$, and $\rho(t, x) > 0$ for all $(t, x) \in [0, 1] \times \mathbb{R}^d$. In addition, ρ solves the transport equation*

$$\partial_t \rho + \nabla \cdot (b \rho) = 0, \quad (2.8)$$

where we defined the velocity

$$b(t, x) = \mathbb{E}(\partial_t I(t, x_0, x_1) + \dot{\gamma}(t)z | x_t = x). \quad (2.9)$$

This velocity is in $C^0([0, 1]; (C^p(\mathbb{R}^d))^d)$ for any $p \in \mathbb{N}$, and such that

$$\forall t \in [0, 1] \quad : \quad \int_{\mathbb{R}^d} |b(t, x)|^2 \rho(t, x) dx < \infty. \quad (2.10)$$

Note that this theorem means that we can write (2.3) as

$$\forall t \in [0, 1] \quad : \quad \int_{\mathbb{R}^d} \phi(x) \rho(t, x) dx = \mathbb{E} \phi(x_t) \quad \text{for any test function } \phi \in C_0^\infty(\mathbb{R}^d), \quad (2.11)$$

The TE (2.8) can be solved either forward in time from the initial condition $\rho(0) = \rho_0$, in which case $\rho(1) = \rho_1$, or backward in time from the final condition $\rho(1) = \rho_1$, in which case $\rho(0) = \rho_0$.

The proof of Theorem 2.6 is given in Appendix B.1; it mostly relies on manipulations involving the characteristic function of the stochastic interpolant x_t . The TE (2.8) for ρ lead to methods for generative modeling and density estimation, as explained in Secs. 2.3 and 2.5, provided that we can estimate the velocity b . This velocity is explicitly available only in special cases, for example when ρ_0 and ρ_1 are both Gaussian mixture densities: this case is treated in Appendix A. In general b must be calculated numerically. In practice, this can be performed via empirical risk minimization of a quadratic objective function, as characterized by our next result:

Theorem 2.7 (Objective). *The velocity b defined in (2.9) is the unique minimizer in $C^0([0, 1]; (C^1(\mathbb{R}^d))^d)$ of the quadratic objective*

$$\mathcal{L}_b[\hat{b}] = \int_0^1 \mathbb{E} \left(\frac{1}{2} |\hat{b}(t, x_t)|^2 - (\partial_t I(t, x_0, x_1) + \dot{\gamma}(t)z) \cdot \hat{b}(t, x_t) \right) dt \quad (2.12)$$

where x_t is defined in (2.1) and the expectation \mathbb{E} is taken independently over $x_0 \sim \rho_0$, $x_1 \sim \rho_1$, and $z \sim \mathbf{N}(0, Id)$.

The proof of Theorem 2.7 is given in Appendix B.1: it relies on the definitions of b in (2.9), as well as the definition of ρ in (2.11) and some elementary properties of the conditional expectation. Interestingly, we also have access to the score of the probability density, as shown by our next result:

Theorem 2.8 (Score). *The score of the probability density ρ specified in Theorem 2.6 is in $C^1([0, 1]; (C^p(\mathbb{R}^d))^d)$ for any $p \in \mathbb{N}$ and given by*

$$s(t, x) = \nabla \log \rho(t, x) = -\gamma^{-1}(t) \mathbb{E}(z | x_t = x) \quad \forall (t, x) \in (0, 1) \times \mathbb{R}^d \quad (2.13)$$

In addition it satisfies

$$\forall t \in [0, 1] \quad : \quad \int_{\mathbb{R}^d} |s(t, x)|^2 \rho(t, x) dx < \infty, \quad (2.14)$$

and is the unique minimizer in $C^1([0, 1]; (C^1(\mathbb{R}^d))^d)$ of the quadratic objective

$$\mathcal{L}_s[\hat{s}] = \int_0^1 \mathbb{E} \left(\frac{1}{2} |\hat{s}(t, x_t)|^2 + \gamma^{-1}(t) z \cdot \hat{s}(t, x_t) \right) dt \quad (2.15)$$

where x_t is defined in (2.1) and the expectation \mathbb{E} is taken independently over $x_0 \sim \rho_0$, $x_1 \sim \rho_1$, and $z \sim \mathbf{N}(0, Id)$

The proof of Theorem 2.8 is given in Appendix B.1. Having access to the score immediately allows us to rewrite the TE (2.8) as forward and backward Fokker-Planck equations, which we state as:

Corollary 2.9 (Fokker Planck equations). *For any $\epsilon \geq 0$, the probability density ρ specified in Theorem 2.6 satisfies:*

1. *The forward Fokker-Planck equation*

$$\partial_t \rho + \nabla \cdot (b_F \rho) = \epsilon \Delta \rho, \quad \rho(0) = \rho_0, \quad (2.16)$$

where we defined the forward drift

$$b_F(t, x) = b(t, x) + \epsilon s(t, x). \quad (2.17)$$

Equation (2.16) is well-posed when solved forward in time from $t = 0$ to $t = 1$, and its solution for the initial condition $\rho(t = 0) = \rho_0$ satisfies $\rho(t = 1) = \rho_1$.

2. *The backward Fokker-Planck equation*

$$\partial_t \rho + \nabla \cdot (b_B \rho) = -\epsilon \Delta \rho, \quad \rho(1) = \rho_1, \quad (2.18)$$

where we defined the backward drift

$$b_B(t, x) = b(t, x) - \epsilon s(t, x). \quad (2.19)$$

Equation (2.18) is well-posed when solved backward in time from $t = 1$ to $t = 0$, and its solution for the final condition $\rho(1) = \rho_1$ satisfies $\rho(0) = \rho_0$.

In Section 2.3 we will use the results of this theorem to design generative models based on forward and backward stochastic differential equations.

Let us make a few remarks about the statements made so far:

Remark 2.10. If we set $\gamma(t) = 0$ in x_t (i.e we remove the latent variable), the stochastic interpolant (2.1) reduces to the one originally considered in [1]. In this setup, the results above formally stand except that we cannot guarantee the spatial regularity of $b(t, x)$ and $s(t, x)$ in general, since this regularity relies on the presence of the latent variable (as shown in the proof of Theorem 2.6). Therefore, the introduction latent variable $\gamma(t)z$ will help at the level of generative models (see Section 2.3), where the solution to ODE/SDE will be better behaved, and at the level of statistical approximation, since the target b and s will be more regular. We will see in Section 3 that it also gives us much greater flexibility in the way we can bridge ρ_0 and ρ_1 and therefore design generative models with appealing properties.

Remark 2.11. We will see in Section 2.4 that the forward and backward FPE in (2.16) and (2.18) are more robust than the TE in (2.8) against approximation errors in the velocity b and the score s , which has practical implications for the generative models based on these equations.

Remark 2.12. We could also obtain $b(t, \cdot)$ at any $t \in [0, 1]$ by minimizing

$$\mathbb{E} \left(\frac{1}{2} |\hat{b}(t, x_t)|^2 - (\partial_t I(t, x_0, x_1) + \dot{\gamma}(t)z) \cdot \hat{b}(t, x_t) \right) \quad t \in [0, 1] \quad (2.20)$$

and $s(t, \cdot)$ at any $t \in (0, 1)$ by minimizing

$$\mathbb{E} \left(\frac{1}{2} |\hat{s}(t, x_t)|^2 + \gamma^{-1}(t)z \cdot \hat{s}(t, x_t) \right) \quad t \in (0, 1) \quad (2.21)$$

Using the time-integrated versions of these objectives given in (2.12) and (2.15) is more convenient numerically as it allows one to parameterize \hat{b} and \hat{s} globally for $(t, x) \in [0, 1] \times \mathbb{R}^d$.

Remark 2.13. From (2.9) we can write

$$b(t, x) = v(t, x) - \dot{\gamma}(t)\gamma(t)s(t, x), \quad (2.22)$$

where s is the score given in (2.13) and we defined the velocity field

$$v(t, x) = \mathbb{E}(\partial_t I(t, x_0, x_1) | x_t = x). \quad (2.23)$$

The velocity field $v \in C^0([0, 1]; (C^p(\mathbb{R}^d))^d)$ for any $p \in \mathbb{N}$ and can be characterized as the unique minimizer of

$$\mathcal{L}_v[\hat{v}] = \int_0^1 \mathbb{E} \left(\frac{1}{2} |\hat{v}(t, x_t)|^2 - \partial_t I(t, x_0, x_1) \cdot \hat{v}(t, x_t) \right) dt \quad (2.24)$$

Learning this velocity and the score separately may be useful in practice.

Remark 2.14. The objectives in (2.12) and (2.15) (as well as the one in (2.24)) are amenable to empirical estimation if we have samples from ρ_0 and ρ_1 , since in that case we can easily generate samples of $x_t = I(t, x_0, x_1) + \gamma(t)z$ at any time $t \in [0, 1]$. We will use this feature in the numerical experiments presented below.

Remark 2.15. Since s is the score of ρ , an alternative objective to estimate it is [21]

$$\int_0^1 \mathbb{E} (|\hat{s}(t, x_t)|^2 + 2\nabla \cdot \hat{s}(t, x_t)) dt. \quad (2.25)$$

The derivation of (2.25) is standard: for the reader's convenience we recall it at the end of Appendix B.1. The advantage of using (2.15) over (2.25) is that it does not requires us to take the divergence of \hat{s} .

2.3 Generative models

Our next result is a direct consequence of Theorem 2.6, and it shows how to design generative models using the stochastic processes associated with the TE (2.8), the forward FPE (2.16), and the backward FPE (2.18):

Corollary 2.16 (Generative models). *At any time $t \in [0, 1]$, the law of the stochastic interpolant x_t coincides with the law of the three processes X_t , X_t^F , and X_t^B , respectively defined as:*

1. *The solutions of the ordinary differential equation (ODE) (aka probability flow) associated with the transport equation (2.8)*

$$\frac{d}{dt}X_t = b(t, X_t), \quad (2.26)$$

solved either forward in time from the initial data $X_{t=0} \sim \rho_0$ or backward in time from the final data $X_{t=1} = x_1 \sim \rho_1$.

2. *The solutions of the forward SDE associated with the FPE (2.16)*

$$dX_t^F = b_F(t, X_t^F)dt + \sqrt{2\epsilon}dW_t, \quad (2.27)$$

solved forward in time from the initial data $X_{t=0}^F \sim \rho_0$ independent of W .

3. *The solutions of the backward SDE associated with the backward FPE (2.18)*

$$dX_t^B = b_B(t, X_t^B)dt + \sqrt{2\epsilon}dW_t^B, \quad W_t^B = -W_{1-t}, \quad (2.28)$$

solved backward in time from the final data $X_{t=1}^B \sim \rho_1$ independent of W^B .

Reverse Itô Calculus. Here, the solution of the reverse-time SDE (2.28) is by definition $X_t^B = Z_{1-t}^F$ where Z_t^F satisfies

$$dZ_t^F = -b_B(1-t, Z_t^F)dt + \sqrt{2\epsilon}dW_t, \quad (2.29)$$

solved forward in time from the initial data $Z_{t=0}^F \sim \rho_1$ independent of W . To avoid repeated application of the transformation $t \rightarrow 1-t$, it is convenient to work with (2.28) directly using

1. For any $f \in C^1([0, 1]; C_0^2(\mathbb{R}_d))$ and $t \in [0, 1]$, the backward Itô formula holds

$$df(t, X_t^B) = \partial_t f(t, X_t^B)dt + \nabla f(X_t^B)dX_t^B - \epsilon \Delta f(t, X_t^B)dt. \quad (2.30)$$

2. For any $g \in C^0([0, 1]; (C_0^0(\mathbb{R}_d))^d)$ and $t \in [0, 1]$, the following backward Itô isometries hold:

$$\mathbb{E}_B^x \int_t^1 g(t, X_t^B) \cdot dW_t^B = 0; \quad \mathbb{E}_B^x \left| \int_t^1 g(t, X_t^B) \cdot dW_t^B \right|^2 = \int_t^1 \mathbb{E}_B^x |g(t, X_t^B)|^2 dt, \quad (2.31)$$

where \mathbb{E}_B^x denotes expectation conditioned on the event $X_{t=1}^B = x$.

These rules are elucidated in the proof of Corollary 2.16 given in Appendix B.2.

The relevance of Corollary 2.16 for generative modeling is clear. Assuming, for example, that ρ_0 is a simple density that can be sampled easily (e.g. a Gaussian or a Gaussian mixture density), we can use the ODE (2.26) or the SDE (2.27) to push these samples forward in time and generate samples from a complex target density ρ_1 . In Section 2.5, we will show how to use the ODE (2.26) or the reverse SDE (2.28) to estimate ρ_1 and $\log \rho_1$ at any $x \in \mathbb{R}^d$ assuming that we can evaluate ρ_0 at any $x \in \mathbb{R}^d$. We will also show how similar ideas can be used to estimate the cross entropy between ρ_0 and ρ_1 .

Remark 2.17. We stress that the stochastic interpolant x_t , the solution X_t to the ODE (2.26), and the solutions X_t^F and X_t^B of the forward and backward SDEs (2.27) and (2.28) are *different* stochastic processes, but their laws all coincide with $\rho(t)$ at any time $t \in [0, 1]$. This is all that matters when applying these processes as generative models. However, the fact that these processes are different has implications for the accuracy of the numerical integration used to sample from them at any t as well as for the propagation of statistical errors (see also the next remark).

Remark 2.18. The generative models based on X_t to the ODE (2.26), and the solutions X_t^F and X_t^B of the forward and backward SDEs (2.27) and (2.28) will typically involve drifts b , b_F , and b_B that are, in practice, imperfectly estimated via minimization of (2.12) and (2.15). It is therefore important to estimate the error such imperfections induces, and how they depend on the generative model used, which is the object of our next section.

2.4 Likelihood control

In this section, we demonstrate that jointly minimizing the objective functions (2.24) and (2.15) (or minimizing the single loss (2.12)) minimizes the KL-divergence from the target density ρ_1 to the model density $\hat{\rho}_1$. The derivation is based on a simple and exact characterization of the KL-divergence between two transport equations or two Fokker-Planck equations with different drifts. Remarkably, we find that the presence of a diffusive term determines whether or not it is sufficient to learn the drift to control KL. This can be seen as a generalization of the result for score-based diffusion models described in [40] to arbitrary generative models described by ODEs or SDEs. The proofs of the statements in this section are provided in Appendix B.3.

We first characterize the KL divergence between two densities transported by two different continuity equations but initialized from the same initial condition:

Lemma 2.19. *Let $\rho_0 : \mathbb{R}^d \rightarrow \mathbb{R}_{\geq 0}$ denote a fixed base probability density function. Given two velocity fields $b, \hat{b} \in C^0([0, 1], (C^1(\mathbb{R}^d))^d)$, let the time-dependent densities $\rho : [0, 1] \times \mathbb{R}^d \rightarrow \mathbb{R}_{\geq 0}$ and $\hat{\rho} : [0, 1] \times \mathbb{R}^d \rightarrow \mathbb{R}_{\geq 0}$ denote the solutions to the transport equations*

$$\begin{aligned} \partial_t \rho + \nabla \cdot (b\rho) &= 0, & \rho(0) &= \rho_0, \\ \partial_t \hat{\rho} + \nabla \cdot (\hat{b}\hat{\rho}) &= 0, & \hat{\rho}(0) &= \rho_0. \end{aligned} \quad (2.32)$$

Then, the Kullback-Leibler divergence of $\rho(1)$ from $\hat{\rho}(1)$ is given by

$$\text{KL}(\rho(1) \parallel \hat{\rho}(1)) = \int_0^1 \int_{\mathbb{R}^d} (\nabla \log \hat{\rho}(t, x) - \nabla \log \rho(t, x)) \cdot (\hat{b}(t, x) - b(t, x)) \rho(t, x) dx dt. \quad (2.33)$$

Lemma 2.19 shows that it is insufficient in general to match \hat{b} with b to obtain control on the KL divergence. The essence of the problem is that a small error in $\hat{b} - b$ does not ensure control on the Fisher divergence $\text{FI}(\rho(t) \parallel \hat{\rho}(t)) = \int_{\mathbb{R}^d} |\nabla \log \rho(t, x) - \nabla \log \hat{\rho}(t, y)|^2 \rho(t, x) dx$, which is necessary due to the presence of $(\nabla \log \hat{\rho} - \nabla \log \rho)$.

In the next lemma, we study the case for two Fokker-Planck equations, and highlight that the situation becomes quite different.

Lemma 2.20. *Let $\rho_0 : \mathbb{R}^d \rightarrow \mathbb{R}_{\geq 0}$ denote a fixed base probability density function. Given two velocity fields $b_F, \hat{b}_F \in C^0([0, 1], (C^1(\mathbb{R}^d))^d)$, let the time-dependent densities $\rho : [0, 1] \times \mathbb{R}^d \rightarrow \mathbb{R}_{\geq 0}$ and $\hat{\rho} : [0, 1] \times \mathbb{R}^d \rightarrow \mathbb{R}_{\geq 0}$ denote the solutions to the Fokker-Planck equations*

$$\begin{aligned} \partial_t \rho + \nabla \cdot (b_F \rho) &= \epsilon \Delta \rho, & \rho(0) &= \rho_0, \\ \partial_t \hat{\rho} + \nabla \cdot (\hat{b}_F \hat{\rho}) &= \epsilon \Delta \hat{\rho}, & \hat{\rho}(0) &= \rho_0. \end{aligned} \quad (2.34)$$

Then, the Kullback-Leibler divergence from $\rho(1)$ to $\hat{\rho}(1)$ is given by

$$\begin{aligned} \text{KL}(\rho(1) \parallel \hat{\rho}(1)) &= \int_0^1 \int_{\mathbb{R}^d} (\nabla \log \hat{\rho}(t, x) - \nabla \log \rho(t, x)) \cdot (\hat{b}_F(t, x) - b_F(t, x)) \rho(t, x) dx dt \\ &\quad - \epsilon \int_0^1 \int_{\mathbb{R}^d} |\nabla \log \rho(t, x) - \nabla \log \hat{\rho}(t, x)|^2 \rho(t, x) dx dt, \end{aligned} \quad (2.35)$$

and as a result

$$\text{KL}(\rho(1) \parallel \hat{\rho}(1)) \leq \frac{1}{\epsilon} \int_0^1 \int_{\mathbb{R}^d} \left| \hat{b}_F(t, x) - b_F(t, x) \right|^2 \rho(t, x) dx dt. \quad (2.36)$$

Lemma 2.20 shows that, unlike for transport equations, the KL-divergence between the solutions of two Fokker-Planck equations is controlled by the error in their drifts. The diffusive term in each Fokker-Planck equations provides an additional negative term in the KL-divergence, which eliminates the need for explicit control on the Fisher divergence.

Putting the above results together, we can state the following result, which demonstrates that the losses (2.12) and (2.15) control the likelihood for learned approximations to the FPE (2.16).

Theorem 2.21. *Let ρ denote the solution of the Fokker-Planck equation (2.16). Given two velocity fields $\hat{b}, \hat{s} \in C^0([0, 1], C^1(\mathbb{R}^d, \mathbb{R}^d))$, define*

$$\hat{b}_F(t, x) = \hat{b}(t, x) + \epsilon \hat{s}(t, x), \quad \hat{v}(t, x) = \hat{b}(t, x) + \gamma(t) \dot{\gamma}(t) \hat{s}(t, x) \quad (2.37)$$

where the function γ satisfies the properties listed in Definition 2.1. Let $\hat{\rho}$ denote the solution to the Fokker-Planck equation

$$\partial_t \hat{\rho} + \nabla \cdot (\hat{b}_F \hat{\rho}) = \epsilon \Delta \hat{\rho}, \quad \hat{\rho}(0) = \rho_0. \quad (2.38)$$

Then,

$$\text{KL}(\rho_1 \parallel \hat{\rho}(1)) \leq \frac{1}{2\epsilon} \left(\mathcal{L}_b[\hat{b}] - \min_{\hat{b}} \mathcal{L}_b[\hat{b}] \right) + \frac{\epsilon}{2} \left(\mathcal{L}_s[\hat{s}] - \min_{\hat{s}} \mathcal{L}_s[\hat{s}] \right), \quad (2.39)$$

where $\mathcal{L}_b[\hat{b}]$ and $\mathcal{L}_s[\hat{s}]$ are the objective functions defined in (2.12) and (2.15), and

$$\text{KL}(\rho_1 \parallel \hat{\rho}(1)) \leq \frac{1}{2\epsilon} \left(\mathcal{L}_v[\hat{v}] - \min_{\hat{v}} \mathcal{L}_v[\hat{v}] \right) + \frac{\sup_{t \in [0, 1]} (\gamma(t) \dot{\gamma}(t) + \epsilon)^2}{2\epsilon} \left(\mathcal{L}_s[\hat{s}] - \min_{\hat{s}} \mathcal{L}_s[\hat{s}] \right). \quad (2.40)$$

where $\mathcal{L}_v[\hat{v}]$ is the objective function defined in (2.24).

Remark 2.22 (Generative modeling). The above results have practical ramifications for generative modeling. In particular, they show that minimizing either the losses (2.12) and (2.15) or (2.24) and (2.15) maximize the likelihood of the stochastic generative model

$$d\hat{X}_t^F = \left(\hat{b}(t, \hat{X}_t^F) + \epsilon \hat{s}(t, \hat{X}_t^F) \right) dt + \sqrt{2\epsilon} dW_t, \quad (2.41)$$

but that minimizing the objective (2.12) is insufficient in general to maximize the likelihood of the deterministic generative model

$$\dot{\hat{X}}_t = \hat{b}(t, \hat{X}_t). \quad (2.42)$$

Moreover, they show that, when learning \hat{b} and \hat{s} , the choice of ϵ that minimizes the upper bound is given by

$$\epsilon^* = \left(\frac{\mathcal{L}_b[\hat{b}] - \min_{\hat{b}} \mathcal{L}_b[\hat{b}]}{\mathcal{L}_s[\hat{s}] - \min_{\hat{s}} \mathcal{L}_s[\hat{s}]} \right)^{1/2} \quad (2.43)$$

so that $\epsilon^* > 1$ if the score is learned to higher accuracy than \hat{b} and $\epsilon^* < 1$ in the opposite situation. Note that (2.43) suggests to take $\epsilon = 0$ if \hat{b} is learned perfectly but \hat{s} is not, and send $\epsilon \rightarrow \infty$ in the opposite situation. We stress however that, while taking $\epsilon = 0$ is achievable in practice and simply leads to the ODE (2.26), taking $\epsilon \rightarrow \infty$ is not, as increasing ϵ speeds-up the time scales in the SDE (2.27) and (2.28), thereby making their numerical integration increasingly costly as the time-step must be decreased inverse-proportionally to ϵ .

2.5 Density estimation and cross-entropy calculation

It is well-known that the solution of the TE (2.8) can be expressed in terms of the solution to probability flow ODE (2.26). Specifically we have:

Lemma 2.23. *Given the velocity field $\hat{b} \in C^0([0, 1], (C^1(\mathbb{R}^d))^d)$, let $\hat{\rho}$ satisfy the transport equation*

$$\partial_t \hat{\rho} + \nabla \cdot (\hat{b} \hat{\rho}) = 0, \quad (2.44)$$

and let $X_{s,t}(x)$ solve the ODE

$$\frac{d}{dt} X_{s,t}(x) = b(t, X_{s,t}(x)), \quad X_{s,s}(x) = x, \quad t, s \in [0, 1] \quad (2.45)$$

Then, given the PDFs ρ_0 and ρ_1 :

1. *The solution to (2.44) for the initial condition $\hat{\rho}(0) = \rho_0$ is given at any time $t \in [0, 1]$ by*

$$\hat{\rho}(t, x) = \exp \left(- \int_0^t \nabla \cdot b(\tau, X_{t,\tau}(x)) d\tau \right) \rho_0(X_{t,0}(x)) \quad (2.46)$$

2. *The solution to (2.44) for the final condition $\hat{\rho}(1) = \rho_1$ is given at any time $t \in [0, 1]$ by*

$$\hat{\rho}(t, x) = \exp \left(\int_t^1 \nabla \cdot b(\tau, X_{t,\tau}(x)) d\tau \right) \rho_1(X_{t,1}(x)) \quad (2.47)$$

This lemma is proven in Appendix B.4. Interestingly, we have similar results for the solution of the forward and backward FPE in (2.16) and (2.18). These results use auxiliary forward and backward SDE in which the role of the forward and backward drifts are switched:

Theorem 2.24. *Given $\epsilon > 0$, and two velocity fields $\hat{b}, \hat{s} \in C^0([0, 1], (C^1(\mathbb{R}^d))^d)$, define*

$$\hat{b}_F(t, x) = \hat{b}(t, x) + \epsilon \hat{s}(t, x), \quad \hat{b}_B(t, x) = \hat{b}(t, x) - \epsilon \hat{s}(t, x), \quad (2.48)$$

and let Y_t^F and Y_t^B be the solution of the following forward and backward SDE:

$$dY_t^F = b_B(t, Y_t^F) dt + \sqrt{2\epsilon} dW_t, \quad (2.49)$$

to be solved forward in time from the initial condition $Y_{t=0}^F = x$ independent of W ; and

$$dY_t^B = b_F(t, Y_t^B) dt + \sqrt{2\epsilon} dW_t^B, \quad W_t^B = -W_{1-t}, \quad (2.50)$$

to be solved backward in time from the final condition $Y_{t=1}^B = x$ independent of W^B . Then, given the PDFs ρ_0 and ρ_1 :

1. The solution to the forward FPE

$$\partial \hat{\rho}_F + \nabla \cdot (\hat{b}_F \hat{\rho}_F) = \epsilon \Delta \hat{\rho}_F, \quad \hat{\rho}_F(0) = \rho_0, \quad (2.51)$$

can be expressed at $t = 1$ as

$$\hat{\rho}_F(1, x) = \mathbb{E}_B^x \left(\exp \left(- \int_0^1 \nabla \cdot \hat{b}_F(t, Y_t^B) dt \right) \rho_0(Y_{t=0}^B) \right), \quad (2.52)$$

where \mathbb{E}_B^x denotes expectation on the path of Y_t^B conditional on $Y_{t=1}^B = x$.

2. The solution to the backward FPE

$$\partial \hat{\rho}_B + \nabla \cdot (\hat{b}_B \hat{\rho}_B) = -\epsilon \Delta \hat{\rho}_B, \quad \hat{\rho}_B(1) = \rho_1, \quad (2.53)$$

can be expressed at any $t = 0$ as

$$\hat{\rho}_B(0, x) = \mathbb{E}_F^x \left(\exp \left(\int_0^1 \nabla \cdot \hat{b}_B(t, Y_t^F) dt \right) \rho_1(Y_{t=1}^F) \right), \quad (2.54)$$

where \mathbb{E}_F^x denotes expectation on the path of Y_t^F conditional on $Y_{t=0}^F = x$.

This theorem is proven in Appendix B.4. Note that to generate data from either $\hat{\rho}_F(1)$ or $\hat{\rho}_B(0)$ assuming that we can sample exactly the PDF at the other end, i.e. ρ_0 and ρ_1 respectively, we would still rely on the equivalent of the forward and backward SDE in (2.27) and (2.28), now used with the approximate drifts in (2.48), i.e.

$$d\hat{X}_t^F = \hat{b}_F(t, \hat{X}_t^F)dt + \sqrt{2\epsilon}dW_t, \quad (2.55)$$

and

$$d\hat{X}_t^B = b_B(t, \hat{X}_t^B)dt + \sqrt{2\epsilon}dW_t^B, \quad W_t^B = -W_{1-t}, \quad (2.56)$$

If we solve (2.55) forward in time from initial data $\hat{X}_{t=0}^F \sim \rho_0$, we then have $\hat{X}_{t=1}^F \sim \hat{\rho}_F(1)$ where $\hat{\rho}_F$ is the solution to the forward FPE (2.51). Similarly If we solve (2.56) backward in time from final data $\hat{X}_{t=1}^B \sim \rho_1$, we then have $\hat{X}_{t=0}^B \sim \hat{\rho}_B(0)$ where $\hat{\rho}_B$ is the solution to the backward FPE (2.53).

The results of Lemma 2.23 and Theorem 2.24 can then be used to test the quality of samples generated either by the ODE (2.26), or by the forward and backward SDE (2.27) and (2.28), using the cross entropy as measure. In particular, the following two results are direct consequences of Lemma 2.23 and Theorem 2.24, respectively:

Corollary 2.25. *In the same conditions as in Lemma 2.23, if $\hat{\rho}(0) = \rho_0$, the cross-entropy of $\hat{\rho}(1)$ relative to ρ_1 is given by*

$$\begin{aligned} H(\rho_1 | \hat{\rho}(1)) &= - \int_{\mathbb{R}^d} \log \hat{\rho}(1, x) \rho_1(x) dx \\ &= \mathbb{E}_1 \int_0^1 \nabla \cdot b(\tau, X_{1,\tau}(x_1)) d\tau - \mathbb{E}_1 \log \rho_0(X_{1,0}(x_1)) \end{aligned} \quad (2.57)$$

where \mathbb{E}_1 denotes the expectation on $x_1 \sim \rho_1$. Similarly, if $\hat{\rho}(1) = \rho_1$, the cross-entropy of $\hat{\rho}(0)$ relative to ρ_0 is given by

$$\begin{aligned} H(\rho_0 | \hat{\rho}(0)) &= - \int_{\mathbb{R}^d} \log \hat{\rho}(0, x) \rho_0(x) dx \\ &= -\mathbb{E}_0 \int_0^1 \nabla \cdot b(\tau, X_{0,\tau}(x_0)) d\tau - \mathbb{E}_0 \log \rho_1(X_{0,1}(x_0)) \end{aligned} \quad (2.58)$$

where \mathbb{E}_0 denotes the expectation on $x_0 \sim \rho_0$.

Corollary 2.26. *In the same conditions as in Theorem 2.24, the cross-entropy of $\hat{\rho}_F(1)$ relative to ρ_1 is given by*

$$\begin{aligned} H(\rho_1|\hat{\rho}_F(1)) &= - \int_{\mathbb{R}^d} \log \hat{\rho}_F(1, x) \rho_1(x) dx \\ &= -\mathbb{E}_1 \log \mathbb{E}_B^{x_1} \left(\exp \left(- \int_0^1 \nabla \cdot b_F(t, Y_t^B) dt \right) \rho_0(Y_{t=0}^B) \right), \end{aligned} \quad (2.59)$$

where $\mathbb{E}_B^{x_1}$ denotes the expectation on Y_t^B conditional on $Y_{t=1}^B = x_1$, and \mathbb{E}_1 denotes the expectation on $x_1 \sim \rho_1$. Similarly, the cross-entropy of $\hat{\rho}_B(0)$ relative to ρ_0 is given by

$$\begin{aligned} H(\rho_0|\hat{\rho}_B(0)) &= - \int_{\mathbb{R}^d} \log \hat{\rho}_B(0, x) \rho_0(x) dx \\ &= -\mathbb{E}_0 \log \mathbb{E}_F^{x_0} \left(\exp \left(\int_0^1 \nabla \cdot b_B(t, Y_t^F) dt \right) \rho_1(Y_{t=1}^F) \right), \end{aligned} \quad (2.60)$$

where $\mathbb{E}_B^{x_0}$ denotes the expectation on Y_t^F conditional on $Y_{t=0}^F = x_0$, and \mathbb{E}_0 denotes the expectation on $x_0 \sim \rho_0$.

If in (2.57), (2.58), (2.59), and (2.60) we approximate the expectations \mathbb{E}_0 and \mathbb{E}_1 over ρ_0 and ρ_1 by empirical expectations over data sets from these densities, these equations allow us to cross-validate different approximations of \hat{b} and \hat{s} . They also allow us to compare the cross-entropies of densities evolved by the TE (2.44), or by the forward and backward FPE (2.51) and (2.53).

Remark 2.27. When using (2.59) and (2.60) in practice, taking the log of the expectations $\mathbb{E}_B^{x_1}$ and $\mathbb{E}_F^{x_0}$ may create difficulties. For example, if we want to use Hutchinson's trace estimator to compute the divergences of b_F and b_B , this will introduce a bias. One way to remove this bias is to use Jensen's inequality to exchange the log and the expectation and get the upper bounds

$$H(\rho_1|\hat{\rho}_F(1)) \leq \int_0^1 \mathbb{E}_1 \mathbb{E}_B^{x_1} \nabla \cdot b_F(t, Y_t^B) dt - \mathbb{E}_1 \mathbb{E}_B^{x_1} \log \rho_0(Y_{t=0}^B), \quad (2.61)$$

and

$$H(\rho_0|\hat{\rho}_B(0)) \leq -\mathbb{E}_0 \mathbb{E}_F^{x_0} \int_0^1 \nabla \cdot b_B(t, Y_t^F) dt - \mathbb{E}_0 \mathbb{E}_F^{x_0} \log \rho_1(Y_{t=1}^F). \quad (2.62)$$

It should be stressed, however, that these bounds are not sharp in general. In fact, using calculations similar to the one presented in the proof of Theorem 2.26, we can derive the exact expressions

$$H(\rho_1|\hat{\rho}_F(1)) = \int_0^1 \mathbb{E}_1 \mathbb{E}_B^{x_1} (\nabla \cdot b_F(t, Y_t^B) - \epsilon |\nabla \log \hat{\rho}_F(t, Y_t^B)|^2) dt - \mathbb{E}_1 \mathbb{E}_B^{x_1} \log \rho_0(Y_{t=0}^B), \quad (2.63)$$

and

$$H(\rho_0|\hat{\rho}_B(0)) = -\mathbb{E}_0 \mathbb{E}_F^{x_0} \int_0^1 (\nabla \cdot b_B(t, Y_t^F) + \epsilon |\nabla \log \hat{\rho}_B(t, Y_t^F)|^2) dt - \mathbb{E}_0 \mathbb{E}_F^{x_0} \log \rho_1(Y_{t=1}^F). \quad (2.64)$$

Unfortunately, since $\nabla \log \hat{\rho}_F \neq \hat{s}$ and $\nabla \log \hat{\rho}_B \neq \hat{s}$ in general due to approximation errors, we do not know how to estimate the extra terms at the right hand side of (2.63) and (2.64). A possibility is to use \hat{s} as proxy to approximate $\nabla \log \rho_F$ and $\nabla \log \rho_B$ but this approximation is uncontrolled.

3 Design considerations

In this section, we discuss how to design the stochastic interpolant x_t defined in (2.1), focusing in particular on how the choice of the functions $I(t, x_0, x_1)$ and $\gamma(t)$ impacts the time-dependent

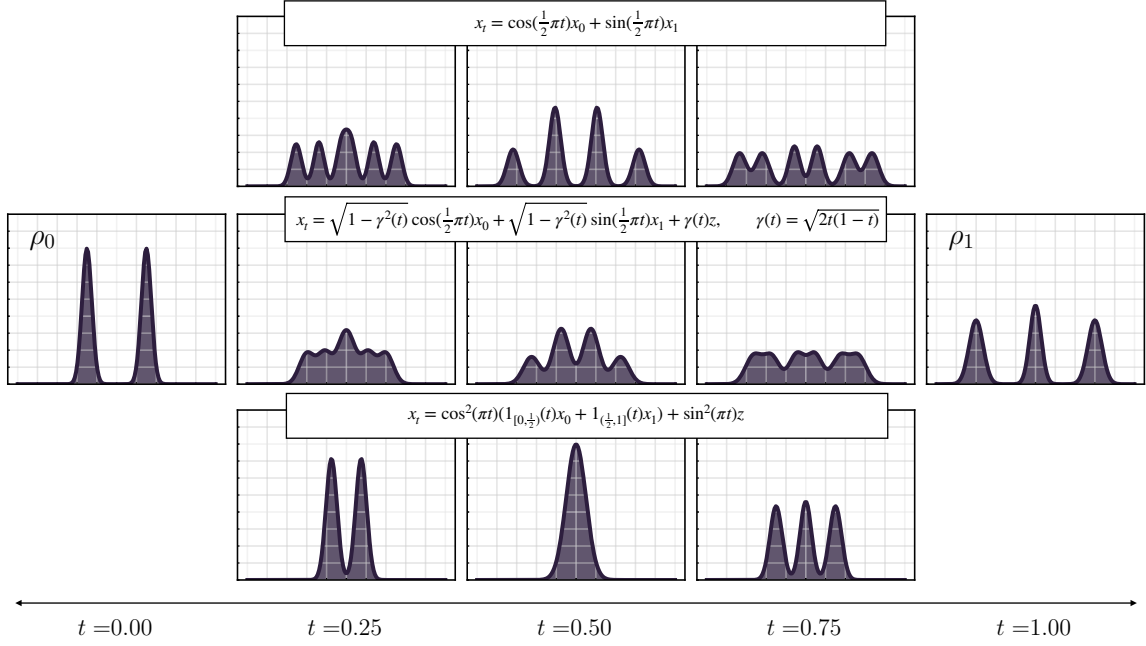


Figure 3: **The effect of $\gamma(t)$ on $\rho(t)$.** A visualization of how the choice of $\gamma(t)$ changes the density $\rho(t)$ of $x_t = \alpha(t)x_0 + \beta(t)x_1 + \gamma(t)z$ when ρ_0 and ρ_1 are Gaussian mixture densities with two modes and three modes, respectively. The first row depicts $\gamma(t) = 0$, which reduces to the stochastic interpolant developed in [1]. This case forms a valid transport between ρ_0 and ρ_1 , but produces spurious intermediate modes in $\rho(t)$. The second row depicts the choice of $\gamma(t) = \sqrt{2t(1-t)}$. In this case, the spurious modes are partially damped by the addition of the latent variable, leading to a simpler $\rho(t)$. The final row shows the Gaussian encoding-decoding, which smoothly encodes ρ_0 into a standard normal distribution on the time interval $[0, 1/2]$, which is then decoded into ρ_1 on the interval $(1/2, 1]$. In this case, no intermediate modes form in $\rho(t)$: the two modes in ρ_0 collide to form $N(0, 1)$ at $t = \frac{1}{2}$, which then spreads into the three modes of ρ_1 . A visualization of individual sample trajectories of deterministic and stochastic generative models based on ODE and SDE whose solutions have these $\rho(t)$ as density can be seen in Figure 6.

density $\rho(t)$ that bridges ρ_0 and ρ_1 . The discussion highlights how the presence of the latent variable $\gamma(t)z$ can simplify the structure of the intermediate density $\rho(t)$, and how it leads to greater design flexibility. Since our ultimate aim is to investigate the properties practical generative models built upon ODEs or on forward and backward SDEs, we will also study the effect of the parameter ϵ that controls the amplitude of the noise in a generative SDE. Finally, the results in this section will allow us to make connections with score-based diffusion models, as well as the rectification procedure introduced in [30]. Throughout, to build intuition, we choose ρ_0 and ρ_1 to be Gaussian mixture densities, for which the drift coefficients can be computed analytically (see Appendix A). This enables us to visualize the effect of each choice on the resulting generative models.

3.1 Spatially linear interpolants

If we make the dependence of $I(t, x_0, x_1)$ on (x_0, x_1) complicated, it becomes difficult to specify *a priori*, and may be preferable to optimize as discussed in Section 4. As a simpler starting point, it is natural to consider a class of functions I that is linear in both x_0 and x_1 , i.e.

$$x_t = \alpha(t)x_0 + \beta(t)x_1 + \gamma(t)z, \quad (3.1)$$

where $\alpha, \beta, \gamma^2 \in C^2([0, 1])$, $\gamma \in C^1((0, 1))$, and satisfy

$$\begin{aligned} \alpha(0) = \beta(1) = 1; \quad \alpha(1) = \beta(0) = \gamma(0) = \gamma(1) = 0; \\ \forall t \in [0, 1] : \alpha(t) \geq 0, \dot{\alpha}(t) \leq 0, \beta(t) \geq 0, \dot{\beta}(t) \geq 0, \gamma(t) \geq 0. \end{aligned} \quad (3.2)$$

As we now show, despite its simplicity, this setup offers significant design flexibility.

It is useful to assume that both ρ_0 and ρ_1 have been scaled to have zero mean and identity covariance (which can be achieved in practice, for example, by an affine transformation of the data). In this case, the time-dependent mean and covariance of (3.1) are given by

$$\mathbb{E}x_t = 0, \quad \mathbb{E}[x_t x_t^T] = (\alpha^2(t) + \beta^2(t) + \gamma^2(t))Id. \quad (3.3)$$

Preserving the identity covariance at all times therefore leads to the constraint

$$\forall t \in [0, 1] : \alpha^2(t) + \beta^2(t) + \gamma^2(t) = 1. \quad (3.4)$$

We note that this choice is also sensible if ρ_0 and ρ_1 have covariances that are not the identity but are on a similar scale. In this case we no longer need to enforce (3.4) exactly, and could for example take three functions whose sum of squares is of order one. For definiteness, in the sequel we discuss possible choices that satisfy (3.4) exactly, with the understanding that the corresponding functions α , β , and γ could all be slightly modified without significantly affecting the conclusions.

Linear and trigonometric interpolants. One way to ensure that (3.4) holds while maintaining the influence of ρ_0 and ρ_1 everywhere on $[0, 1]$ except at the endpoints is to choose

$$\alpha(t) = t, \quad \beta(t) = 1 - t, \quad \gamma(t) = \sqrt{2t(1 - t)}. \quad (3.5)$$

This choice leads to the stochastic interpolant specified in (3.1). It is also the choice that was advocated in [30], without the inclusion of the latent variable ($\gamma = 0$). Another possibility that gives more leeway is to pick any $\gamma : [0, 1] \rightarrow [0, 1]$ and set

$$\alpha(t) = \sqrt{1 - \gamma^2(t)} \cos(\tfrac{1}{2}\pi t), \quad \beta(t) = \sqrt{1 - \gamma^2(t)} \sin(\tfrac{1}{2}\pi t). \quad (3.6)$$

With $\gamma = 0$, this was the choice preferred in [1]. As shown in Theorem 2.6, the presence of the latent variable $\gamma(t)z$ for $\gamma \neq 0$ smooths both the density $\rho(t)$ and the velocity b defined in (2.9) spatially, which provides a computational advantage at sample generation time because it simplifies the required numerical integration of (2.26), (2.27), and (2.28). Intuitively, this is because the density $\rho(t)$ of x_t can be represented exactly as the density that would be obtained with $\gamma = 0$ convolved with $N(0, \gamma^2(t)Id)$ at each $t \in (0, 1)$. A comparison between the PDF $\rho(t)$ obtained with trigonometric interpolants with $\gamma(t) = 0$ and $\gamma(t) = \sqrt{2t(1 - t)}$ can be seen in the first and second row of Figure 3.

Gaussian encoding-decoding. Adding the latent variable $\gamma(t)z$ to (2.1) has another potential advantage, in that we can use the density of $\gamma(t)z$ as an intermediate to interpolate between ρ_0 and ρ_1 .

This can be advantageous if ρ_0 and ρ_1 have distinct complex features, which would be duplicated in $\rho(t)$ at intermediate times if not for the smoothing effect of the latent variable; this behavior is seen in Figure 3, where it most

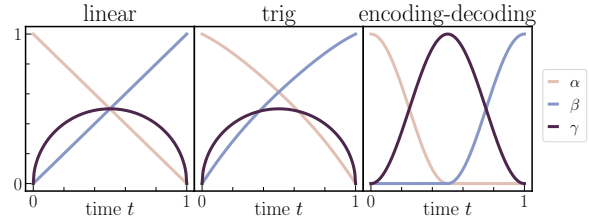


Figure 4: **The functions $\alpha(t)$, $\beta(t)$, and $\gamma(t)$** for the linear (3.5), trigonometric (3.6), and Gaussian encoding-decoding (3.7) interpolants.

$\gamma(t) :$	$\sqrt{at(1-t)}$	$t(1-t)$	$\hat{\sigma}(t)$	$\sin^2(\pi t)$
C^1 at $t = 0, 1$	x	✓	✓	✓

Table 5: **Differentiability of $\gamma(t)$.** A characterization of the possible choices of $\gamma(t)$ with respect to their differentiability. The column specified by $\hat{\sigma}(t)$ is sum of sigmoid functions, made compact by the notation $\hat{\sigma}(t) = \sigma(f(t+1)) - \sigma(f(t-1)) - \sigma(f) + \sigma(-f)$, where $\sigma(t) = e^t/(1+e^t)$ and f is a scaling factor chosen in this case to be $f = 10$.

prominent in the first row with $\gamma(t) = 0$. From a statistical learning perspective, eliminating the formation of spurious features will simplify the estimation of the velocity field b , which becomes smoother as the formation of such features is suppressed. A useful limiting case is to devolve the data from ρ_0 completely into noise by the halfway point $t = \frac{1}{2}$ and to reconstruct ρ_1 completely from noise starting from $t = \frac{1}{2}$. One choice that allows us to do so while satisfying (3.4) is

$$\alpha(t) = \cos^2(\pi t)1_{[0, \frac{1}{2})}(t), \quad \beta(t) = \cos^2(\pi t)1_{(\frac{1}{2}, 1]}(t), \quad \gamma(t) = \sin^2(\pi t), \quad (3.7)$$

where $1_A(t)$ is the indicator function of A , i.e. $1_A(t) = 1$ if $t \in A$ and $1_A(t) = 0$ otherwise. With this choice, it is easy to see that $x_{t=\frac{1}{2}} = \gamma(\frac{1}{2})z \sim \mathcal{N}(0, \gamma^2(\frac{1}{2}))$, which seamlessly glues together two interpolants towards a Gaussian.

Even though the choice (3.7) encodes ρ_0 into pure noise on the interval $[0, \frac{1}{2}]$, which is then decoded into ρ_1 on the interval $[\frac{1}{2}, 1]$ (and vice-versa when proceeding backwards in time), the resulting velocity b still defines a single continuity equation that maps ρ_0 to ρ_1 on $[0, 1]$. This is most clearly seen at the level of the probability flow (2.26), since its solution X_t is a bijection between the initial and final conditions $X_{t=0}$ and $X_{t=1}$, but a similar pairing will also be observed in the solutions to the forward and backward SDEs (2.27) and (2.28), whose solutions at time $t = 1$ or $t = 0$ remain correlated with the initial or final condition used. This allows for a more direct means of image-to-image translation with diffusions as compared to the recent approach described in [43]. The choice (3.7) is depicted in the final row of Figure 3, where no spurious modes form at all; individual sample trajectories of the deterministic and stochastic generative models based on ODE and SDE whose solutions have this $\rho(t)$ as density can be seen in the panels forming the third column in Figure 6.

Unsurprisingly, it is necessary to have $\gamma(t) > 0$ for the choice (3.7): for $\gamma(t) = 0$, the density $\rho(t)$ collapses to a Dirac measure at $t = \frac{1}{2}$. This consideration highlights that the inclusion of the latent variable $\gamma(t)z$ matters even for the deterministic dynamics (2.26), and its presence is distinct from the stochasticity inherent to the SDEs (2.27) and (2.28), that we will discuss in Section 3.2.

The influence of γ on b at $t = 0$ and $t = 1$. Another potential advantage of including the latent variable $\gamma(t)z$ is its impact on the velocity b at the end points. Consider the decomposition of b in (2.22) – for the linear interpolant (3.1), this decomposition can be written

$$b(t, x) = \alpha(t)\mathbb{E}(x_0|x_t = x) + \beta(t)\mathbb{E}(x_1|x_t = x) - \dot{\gamma}(t)\gamma(t)s(t, x), \quad (3.8)$$

where s is the score given in (2.13). Since $x_{t=0} = x_0$ and $x_{t=1} = x_1$, we have

$$\begin{aligned} b(x, 0) &= \dot{\alpha}(0)x + \dot{\beta}(0)m_1 - \lim_{t \rightarrow 0} \gamma(t)\dot{\gamma}(t)s_0(x), \\ b(x, 1) &= \dot{\alpha}(1)m_0 + \dot{\beta}(1)x - \lim_{t \rightarrow 1} \gamma(t)\dot{\gamma}(t)s_1(x), \end{aligned} \quad (3.9)$$

where $m_0 = \mathbb{E}x_0$, $m_1 = \mathbb{E}x_1$, $s_0 = \nabla \log \rho_0$, and $s_1 = \nabla \log \rho_1$. Taking $\gamma \in C^1([0, 1])$, because $\gamma(0) = \gamma(1) = 0$, the terms involving the scores s_0 and s_1 in these expressions vanish. Choosing

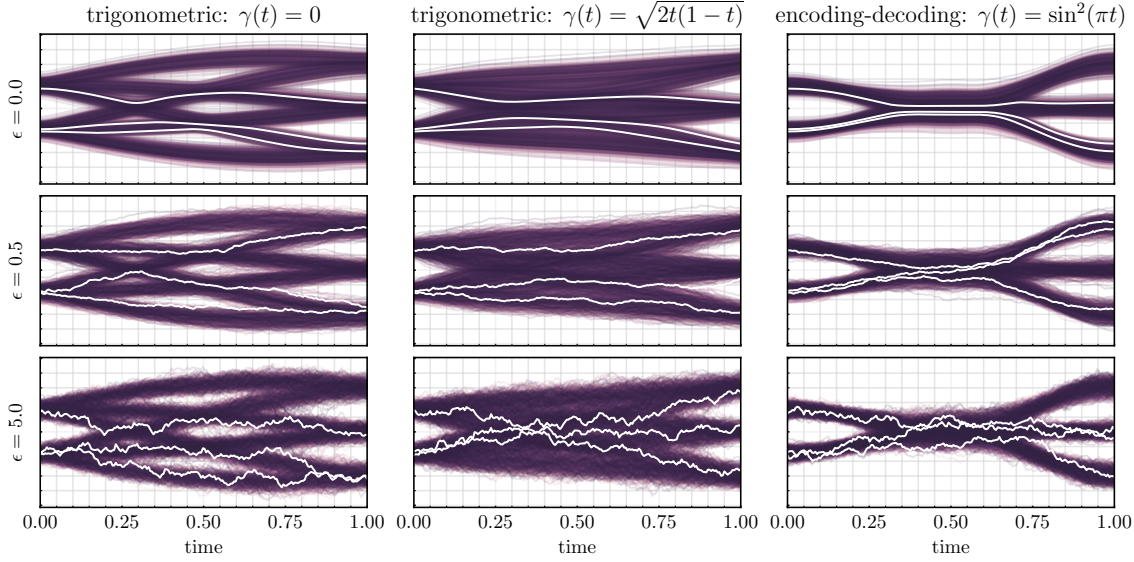


Figure 6: **The effect of ϵ on sample trajectories.** A visualization of how the choice of ϵ affects the sample trajectories obtained by solving the ODE (2.26) or the forward SDE (2.27). The set-up is the same as in Figure 3: ρ_0 and ρ_1 are taken to be the same Gaussian mixture densities as in Figure 3, and the analytical expressions for b and s are used. In the three panels in each column the value of γ is the same, and each panel shows trajectories with different ϵ . Three specific trajectories from the same three initial conditions drawn from ρ_0 are also highlighted in white in every panel. As ϵ increases but γ stays the same, the density $\rho(t)$ is unchanged, but the individual trajectories sampling it become increasingly stochastic. While all choices are equivalent with exact b and s , Theorem 2.21 shows that nonzero values of ϵ provide control on the likelihood in terms of the error in b and s when they are approximate.

$\gamma^2 \in C^2([0, 1])$ but γ not differentiable at $t = 0, 1$ leaves open the possibility that the limits remain nonzero. For example, taking

$$\gamma(t) = \sqrt{at(1-t)}, \quad a < 4 \quad (3.10)$$

we obtain

$$\lim_{t \rightarrow 0} \gamma(t) \dot{\gamma}(t) = - \lim_{t \rightarrow 1} \gamma(t) \dot{\gamma}(t) = \frac{a}{2}. \quad (3.11)$$

As a result, the choice (3.10) ensures that the velocity b encodes information about the score of the densities ρ_0 and ρ_1 at the end points, where $\rho(t)$ must converge to one of them.

Remark 3.1 (Brownian bridge). The choice (3.10) is conceptually interesting, as it corresponds to using a latent variable $\gamma(t)z$ that has the same statistical properties at any fixed $t \in [0, 1]$ as the scaled Brownian bridge $\sqrt{a}B_t$, i.e. the process realizable in terms of the Wiener process W_t as $B_t = W_t - tW_1$, which by definition satisfies $B_1 = B_0 = 0$. Indeed, both $\sqrt{a}B_t \sim \mathcal{N}(0, at(1-t)Id)$ and $\gamma(t)z = \sqrt{at(1-t)}z \sim \mathcal{N}(0, at(1-t)Id)$ for all $t \in [0, 1]$, so that they lead to the same ρ and b .

Other choices of γ . While the choice of $\gamma(t)$ given in (3.10) is appealing because of its nontrivial influence on the velocity b at the endpoints, one is free to explore a variety of alternatives. We present some examples in the table below, specifying the differentiability of γ at $t = 0, 1$. The function $\gamma(t)$ specified in (3.10) is the only case in the presented set for which the score is non-vanishing in the velocity b at the endpoints. In the following section, we illustrate that there are evidential tradeoffs between different gammas, which could be directly related to this fact. When using the ODE as a

generative model versus, the score is only felt through b , whereas it is explicit when using the SDE as a generative model.

3.2 Deterministic vs stochastic generative models

So far, we have been focused on the impact of α , β , and γ in (3.1) on the density $\rho(t)$. However, as shown in Section 2.2, the evolution of this density $\rho(t)$ can be captured exactly by either the transport equation (2.8) or by the forward and backward Fokker-Planck equations (2.16) and (2.18). These perspectives lead to generative models that are either based on the deterministic dynamics (2.26) or the forward and backward stochastic dynamics (2.27) and (2.28), where the intrinsic level of stochasticity can be tuned by varying the value of ϵ . We showed in Section 2.4 that setting $\epsilon > 0$ can offer better control on the likelihood when using an imperfect velocity b and an imperfect score s ; moreover, the optimal choice of ϵ is determined by the relative accuracy of the estimates of b and s . Having laid out the evolution of the density $\rho(t)$ for different choices of γ in the previous section, we show how different values of ϵ can build these densities from individual trajectories independent of the overall level of stochasticity in Figure 6. As ϵ increases, the intrinsic level of stochasticity also increases, but by construction the marginal density $\rho(t)$ for fixed α , β and γ is independent of ϵ .

The roles of $\gamma(t)$ and ϵ for 2D density estimation. We explore these tradeoffs of using different level of latent variable via γ , and using the ODE versus SDE as a generative model for the case where the velocity b is learned over a parametric class defined by feed-forward neural networks. We consider a target density ρ_1 whose mass concentrates on a 2-dimensional checkerboard and a base density $\rho_0 = \mathcal{N}(0, Id)$, with the target chosen based on the hardness of learning a density with fixed boundaries. The same model architecture and training is used to learn both b and s for the variety of choices of γ given in Table 5. The feed-forward network is defined with 4 layers, each of size 512, with ReLU [33] activation functions between each layer. For more experimental specifications, see Appendix C.

After training, we draw 300,000 samples using either the ODE ($\epsilon = 0$) or the SDE under three different noise magnitudes: $\epsilon = 0.5, 1.0, 2.5$. We construct kernel density estimates of each, and compare such to the original stochastic interpolant without a latent variable from [1] as well to the exact density. Results are given in Figure 7 for each γ and each ϵ . Sampling with $\epsilon > 0$ empirically performs better, though the gap is smallest when using the γ specified in (3.10). Moreover, even when $\epsilon = 0$, using the probability flow for this γ performs better than the original interpolant from [1] which used $\gamma(t) = 0$. Numerical comparisons of the mean and variance of the absolute value of the difference of $\log \rho_1$ (exact) from $\log \rho(1)$ (model) for the various configurations are given in Figure 8, which corroborate the above observations.

3.3 One-sided stochastic interpolants for Gaussian ρ_1

We now study the special case $\rho_1 = \mathcal{N}(0, Id)$; this setting is practically relevant, as $\mathcal{N}(0, Id)$ is a common choice of base density for generative modeling in the absence of prior information, and it will allow us to instantiate score-based diffusion within our general framework. In this setting, the effect of the latent variable z can be lumped with x_1 , leading to a simpler type of stochastic interpolant:

Definition 3.2 (One-sided stochastic interpolant). *Given a probability density function $\rho_0 : \mathbb{R}^d \rightarrow \mathbb{R}_{\geq 0}$, a one-sided stochastic interpolant between ρ_0 and $\mathcal{N}(0, Id)$ is a stochastic process y_t*

$$y_t = J(t, x_0) + \beta(t)z, \quad t \in [0, 1] \quad (3.12)$$

that fulfills the requirements:

1. $J : [0, 1] \times \mathbb{R}^d \rightarrow \mathbb{R}^d$ satisfies the boundary conditions $J(0, x_0) = x_0$ and $J(1, x_0) = 0$.

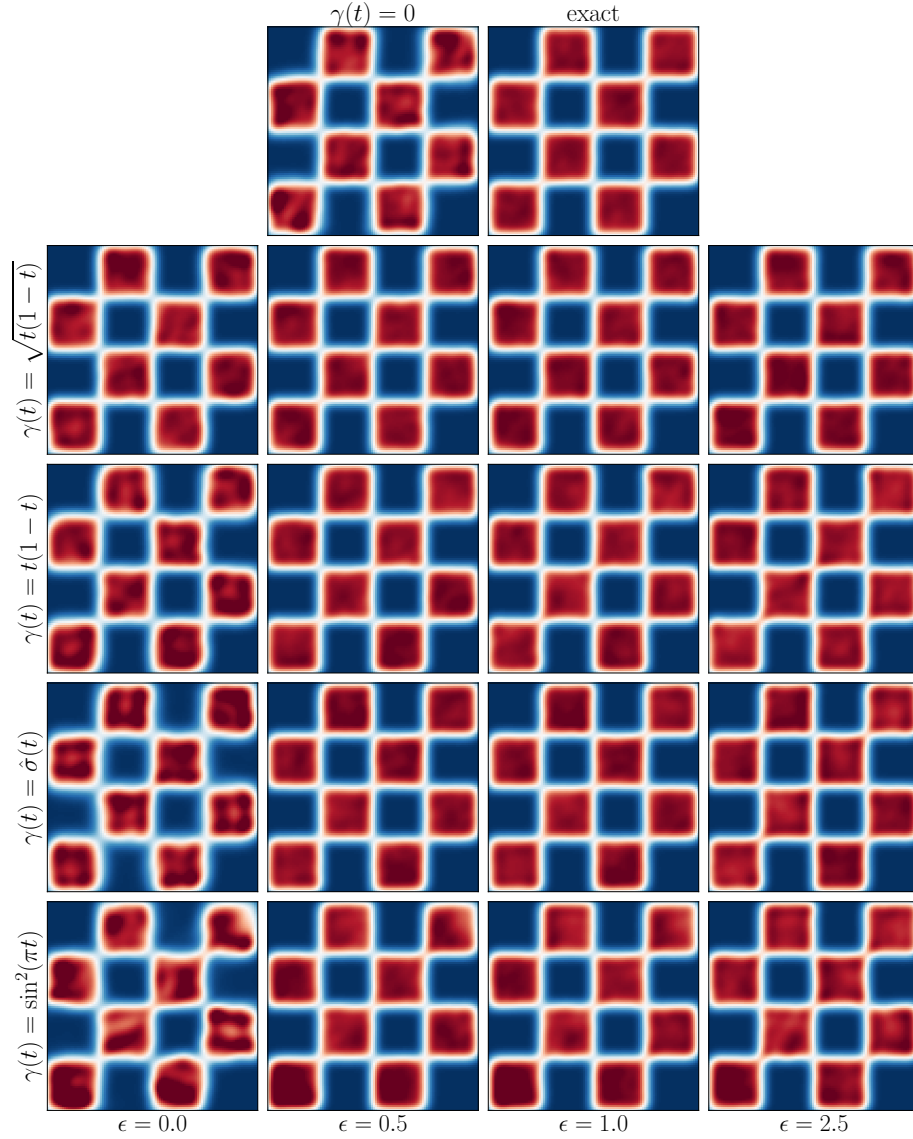


Figure 7: **The effects of $\gamma(t)$ and ϵ on sample quality.** Kernel density estimates for samples drawn from models with different choices of γ and different choices of ϵ . Sampling with $\epsilon = 0$ corresponds to using the probability flow with the learned drift b , whereas sampling with $\epsilon > 0$ corresponds to using the SDE with the learned drift b and score s . We empirically observe that SDE sampling is generically better than ODE sampling for this target density, though the gap is smallest for probability flow specified with $\gamma(t) = \sqrt{t(1-t)}$, in agreement with the remarks in Section 3.1 regarding the influence of γ on b . The SDE performs well at any noise level, though numerically integrating it for higher ϵ requires a smaller step size.

2. x_0 and z are random variables drawn independently from ρ_0 and $N(0, Id)$, respectively.
3. $\beta : [0, 1] \rightarrow \mathbb{R}$ satisfies $\beta(0) = 0$, $\beta(1) = 1$, $\beta(t) > 0$ for all $t \in (0, 1]$, and $\beta^2 \in C^1([0, 1])$.

By construction, $y_{t=0} = x_0 \sim \rho_0$ and $y_{t=1} = z \sim N(0, Id)$, so that the distribution of the

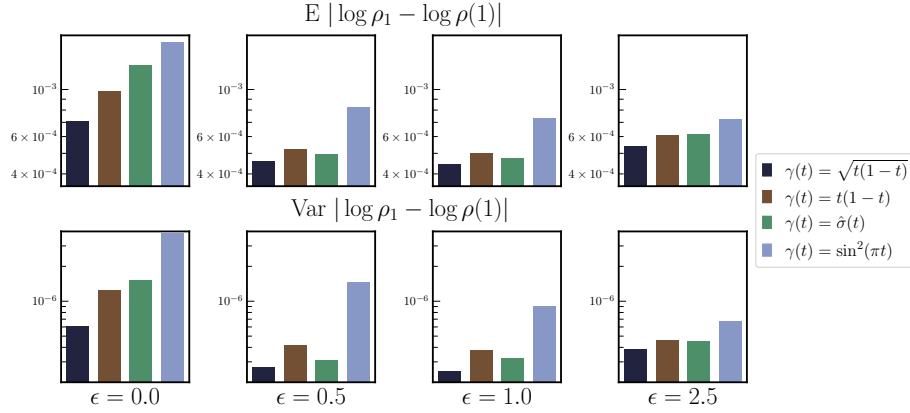


Figure 8: For each γ and each ϵ specified in Figure 7, the mean and variance of the absolute value of the difference of $\log \rho_1$ (exact) from $\log \rho(1)$ (model) is computed. The model specified with $\gamma(t) = \sqrt{t(1-t)}$ is the best performing probability flow ($\epsilon = 0$), though writ large, the SDE sampling with the same learned drift b and score s performs better, complementing the observations in the previous figure.

stochastic process y_t bridges ρ_0 and $\mathcal{N}(0, Id)$. It is easy to see that the one-sided stochastic interpolant defined in (3.12) will have the same density as the stochastic interpolant defined in (2.1) if we set $I(t, x_0, x_1) = J_t(x_0) + \delta(t)x_1$ and take $\delta^2(t) + \gamma^2(t) = \beta^2(t)$. Restricting to this case, our earlier theoretical results apply where the velocity field b defined in (2.9) becomes

$$b(t, x) = \mathbb{E}(\partial_t J(t, x_0) + \dot{\beta}(t)z | y_t = x), \quad (3.13)$$

and the quadratic objective in (2.12) becomes

$$\mathcal{L}_b[\hat{b}] = \int_0^1 \mathbb{E} \left(\frac{1}{2} |\hat{b}(t, y_t)|^2 - \left(\partial_t J(t, x_0) + \dot{\beta}(t)z \right) \cdot \hat{b}(t, y_t) \right) dt. \quad (3.14)$$

In the expression above, y_t is given by (3.12) and the expectation \mathbb{E} is taken independently over $x_0 \sim \rho_0$ and $z \sim \mathcal{N}(0, Id)$. Similarly, the score is given by

$$s(t, x) = -\beta^{-1}(t) \mathbb{E}(z | y_t = x). \quad (3.15)$$

Moreover, we can weaken Assumption 2.5 to the following requirement:

Assumption 3.3. *The density $\rho_0 \in C^2(\mathbb{R}^d)$, satisfies $\rho_0(x) > 0$ for all $x \in \mathbb{R}^d$, and:*

$$\int_{\mathbb{R}^d} |\nabla \log \rho_0(x)|^2 \rho_0(x) dx < \infty. \quad (3.16)$$

The function $J \in C^2([0, 1], C^2(\mathbb{R}^d)^d)$ satisfies

$$\exists C_1 < \infty : \quad |\partial_t J(t, x_0)| \leq C_1 |x_0| \quad \text{for all } (t, x_0) \in [0, 1] \times \mathbb{R}^d, \quad (3.17)$$

and

$$\exists M_1, M_2 < \infty : \quad \mathbb{E}[|\partial_t J(t, x_0)|^4] \leq M_1; \quad \mathbb{E}[|\partial_t^2 J(t, x_0)|^2] \leq M_2, \quad \text{for all } t \in [0, 1], \quad (3.18)$$

where the expectation is taken over $x_0 \sim \rho_0$.

Remark 3.4. The construction above can easily be generalized to the case where $\rho_1 = \mathbf{N}(0, C_1)$ with C_1 a positive-definite matrix. Without loss of generality, we can then assume that C_1 can be represented as $C_1 = \sigma_1 \sigma_1^\top$ where σ_1 is a lower-triangular matrix and replace (3.12)

$$x_t = J(t, x_0) + \beta(t) \sigma_1 z, \quad t \in [0, 1], \quad (3.19)$$

with J and β satisfying the conditions listed in Definition 3.2 and where $z \sim \mathbf{N}(0, Id)$.

3.4 Comparison with score-based diffusion models (SBDM)

SBDMs are based on variants of the Ornstein-Uhlenbeck process

$$dZ_t = -Z_t dt + \sqrt{2} dW_t, \quad Z_{t=0} \sim \rho_0, \quad (3.20)$$

which has the property that the marginal density of its solution at time t converges to a standard normal as t tends towards infinity. By learning the score of the density of Z_t , we can write the associated backward SDE for (3.20), which can then be used as a generative model. Since the solution of (3.20) from the initial condition $Z_{t=0} = x_0$ reads

$$Z_t = x_0 e^{-t} + \sqrt{2} \int_0^t e^{-t+s} dW_s, \quad (3.21)$$

the law of Z_t conditional on $Z_{t=0} = x_0$ is given at any time $t \in [0, \infty)$ by

$$Z_t \sim N(x_0 e^{-t}, (1 - e^{-2t})). \quad (3.22)$$

As a result, the time-dependent density of the OU process in (3.20) coincides with the density of the infinite-horizon one-sided stochastic interpolant

$$y_t = x_0 e^{-t} + \sqrt{1 - e^{-2t}} z, \quad x_0 \sim \rho_0, \quad z \sim \mathbf{N}(0, Id), \quad t \in [0, \infty). \quad (3.23)$$

Infinite-horizon. The above stochastic interpolant does not satisfy some of the properties that we impose in this paper – namely, the density of y_t only converges to $\mathbf{N}(0, Id)$ as $t \rightarrow \infty$. In SBDM, this is handled by capping the evolution of Z_t on a finite time interval $[0, T]$ with $T < \infty$ and using the backward SDE associated with (3.20) restricted to $[0, T]$. However, this introduces an additional source of error that is not present with the finite-time one-sided interpolation procedure introduced here, because the final conditions used for the backward SDE are drawn from $\mathbf{N}(0, Id)$ even though the density of the process (3.20) is not exactly Gaussian at time T .

One-sided stochastic interpolants have the advantage that they can be used on $t \in [0, 1]$ without bias. The price paid is that we need to learn the velocity field b defined in (3.13) via minimization of the objective (3.14) in addition to the score in order to use the backward SDE (2.28) as a generative model (note that using the ODE (2.26) only requires learning b). Using two-sided stochastic interpolants offers the additional advantage that ρ_1 can be any density, not just $\mathbf{N}(0, Id)$.

SBDM in finite time. Interestingly, when the function $J(t, x_0)$ is linear in x_0 , the finite-horizon one-sided stochastic interpolant satisfies a closed forward SDE:

Theorem 3.5. *Consider the finite-horizon one-sided stochastic interpolant*

$$y_t = \alpha(t) x_0 + \beta(t) z, \quad (3.24)$$

with x_0 and z drawn independently from ρ_0 and $\mathbf{N}(0, Id)$, respectively, and where the functions α and β^2 are in $C^1([0, 1])$ and satisfy

$$\alpha(0) = \beta(1) = 1; \quad \alpha(1) = \beta(0) = 0; \quad \forall t \in (0, 1) : \alpha(t) > 0, \dot{\alpha}(t) < 0, \beta(t) > 0, \dot{\beta}(t) < 0. \quad (3.25)$$

Then at any time $t \in [0, 1)$, the law of y_t coincides with the law of the solution to the forward SDE

$$dZ_t^F = \alpha^{-1}(t)\dot{\alpha}(t)Z_t^F dt + \sqrt{2D(t)}dW_t, \quad Z_{t=0}^F \sim \rho_0, \quad (3.26)$$

where we defined

$$D(t) = \beta(t)\dot{\beta}(t) - \beta^2(t)\alpha^{-1}(t)\dot{\alpha}(t). \quad (3.27)$$

The proof is given in Appendix B.5. The conditions in (3.2) guarantee that the diffusion coefficient $D(t)$ is positive for $t \in [0, 1]$. If we instead consider the infinite time interval $[0, \infty)$ and choose $\alpha(t) = e^{-t}$ and $\beta(t) = \sqrt{1 - e^{-2t}}$ as in (3.21), a direct calculation shows that the SDE (3.26) reduces to the OU process in (3.20).

The result of Theorem 3.5 indicates that if we learn the score for the linear one-sided stochastic interpolant in (3.24), e.g. via minimization of the objective in (2.15), we can use the solution to the following backward SDE as a generative model

$$dZ_t^B = \alpha^{-1}(t)\dot{\alpha}(t)Z_t^B dt - 2D(t)s(t, Z_t^B)dt + \sqrt{2D(t)}dW_t^B, \quad Z_{t=1}^B \sim \mathcal{N}(0, Id). \quad (3.28)$$

However, the difficulty with this backward SDE (as well as the forward SDE (3.26) if we want to extend its solution until $t = 1$) is that, due to the boundary condition $\alpha(1) = 0$ and $\alpha \in C^1([0, 1])$, we necessarily have

$$\alpha^{-1}(t)\dot{\alpha}(t) = -(1-t)^{-1} + O(1), \quad D(t) = (1-t)^{-1} + O(1) \quad \text{as } t \rightarrow 1, \quad (3.29)$$

so that the drift and the diffusion coefficients in (3.26) and (3.28) are singular at $t = 1$.

Remark 3.6 (Non-singularity for stochastic interpolants). Unlike finite-time SBDM, the drifts in the ODE and the forward and backward SDEs listed in Theorem (2.16) are non-singular. In fact, if we write the forward SDE (3.26) as a probability flow ODE, i.e. (going back to denoting as X_t the solution to be consistent with the notation of Section 2

$$\frac{d}{dt}X_t = \alpha^{-1}(t)\dot{\alpha}(t)X_t - D(t)s(t, X_t), \quad (3.30)$$

the right-hand side of this equation is precisely the drift $b \in C^0([0, 1], C^1(\mathbb{R}^d)^d)$ defined in (2.9) with $I(t, x_0, x_1) = \alpha(t)x_0 + \beta(t)x_1$, and hence it is well-defined and continuous at $t = 0$ and $t = 1$:

$$\lim_{t \rightarrow 0} \alpha^{-1}(t)\dot{\alpha}(t)x - D(t)s(t, x) = b(0, x), \quad \lim_{t \rightarrow 1} \alpha^{-1}(t)\dot{\alpha}(t)x - D(t)s(t, x) = b(1, x). \quad (3.31)$$

A better way to take advantage of the extra stability conferred by using stochastic models instead of deterministic ones is to turn the ODE (3.30) into forward and backward SDEs, i.e. to pick some $\epsilon > 0$ and use

$$dX_t^F = \alpha^{-1}(t)\dot{\alpha}(t)X_t^F dt + (\epsilon - D(t))s(t, X_t^F)dt + \sqrt{2\epsilon}dW_t, \quad (3.32)$$

and

$$dX_t^B = \alpha^{-1}(t)\dot{\alpha}(t)X_t^B dt - (\epsilon + D(t))s(t, X_t^B)dt + \sqrt{2\epsilon}dW_t^B. \quad (3.33)$$

3.5 Rectifying stochastic interpolants

Our approach offers a way to apply the rectifying procedure proposed in [30], but without introducing any bias. Let us discuss this in the context of one-sided stochastic interpolants where the procedure is simpler. Suppose that we started with some $J(t, x_0)$ and have used it to learn b via minimization of (3.14). Denote by $X_t(x_0)$ the solution to the ODE (2.26) with this b and the initial condition $X_{t=0}(x_0) = x_0$, i.e.

$$\frac{d}{dt}X_t(x_0) = b(t, X_t(x_0)), \quad X_{t=0}(x_0) = x_0. \quad (3.34)$$

If we pick new function α and β satisfying the conditions in (3.2), we can then define a new one-sided interpolant using

$$y_t = \alpha(t)X_t(x_0) + \beta(t)z \quad (3.35)$$

Clearly, we have $y_{t=0} = x_0 \sim \rho_0$ and $y_{t=1} = z \sim \mathbf{N}(0, Id)$ since $X_{t=0}(x_0) = x_0$. We can then learn a new velocity b via minimizing (3.14) again using the new interpolant. This rectification procedure is similar to the one proposed in [30], except that it is unbiased, since (3.35) is a valid one-sided interpolant that satisfies all the conditions of Definition 3.2. The procedure could also be iterated upon. While it adds cost to the learning, the benefit is that it will lead to simpler flows, which was the original motivation of [30].

A similar procedure can also be applied to the original (two-sided) interpolant. For the sake of brevity we will not discuss it, but rather focus on an alternative procedure that allows us to calculate Schrödinger bridges.

4 Stochastic interpolants and Schrödinger bridges

In the section, we show how our framework can be used to solve the Schrödinger bridge problem. For background material on this problem, we refer the reader e.g. to [27]. Consistent with the overall viewpoint of this paper, we consider the fluid dynamics formulation of the Schrödinger bridge problem in which one focus on finding a pair PDF/velocity, (ρ, u) , that solve the following optimization problem (here $\epsilon > 0$)

$$\begin{aligned} & \min \int_0^1 \int_{\mathbb{R}^d} |\nabla \hat{u}(t, x)|^2 \hat{\rho}(t, x) dx dt \\ & \text{subject to: } \partial_t \hat{\rho} + \nabla \cdot (\hat{u} \hat{\rho}) = \epsilon \Delta \hat{\rho}, \quad \hat{\rho}(0) = \rho_0 \quad \hat{\rho}(1) = \rho_1 \end{aligned} \quad (4.1)$$

Under our assumptions on ρ_0, ρ_1 listed in Assumption 2.5, it is known (see e.g. Proposition 4.1 in [27]) that problem (4.1) has a unique minimizer $(\rho, u = \nabla \lambda)$, with (ρ, λ) classical solutions of the Euler-Lagrange equations:

$$\begin{aligned} \partial_t \rho + \nabla \cdot (\nabla \lambda \rho) &= \epsilon \Delta \rho, & \rho(0) &= \rho_0, & \rho(1) &= \rho_1, \\ \partial_t \lambda + \frac{1}{2} |\nabla \lambda|^2 &= -\epsilon \Delta \lambda. \end{aligned} \quad (4.2)$$

To proceed we will make the additional assumption that the solution ρ to (4.2) can be reversibly mapped to a standard Gaussian:

Assumption 4.1. *There exists of a reversible map $T : [0, 1] \times \mathbb{R}^d \rightarrow \mathbb{R}^d$ with $T, T^{-1} \in C^1([0, 1], (C^d(\mathbb{R}^d))^d)$ such that:*

$$\forall t \in [0, 1] \quad : \quad z \sim \mathbf{N}(0, Id) \Rightarrow T(t, z) \sim \rho(t); \quad x_t \sim \rho(t) \Rightarrow T^{-1}(t, x_t) \sim \mathbf{N}(0, Id), \quad (4.3)$$

where ρ is the solution to (4.2).

We stress that the actual form of the map T is not important for the arguments below. Assumption 4.1 can be used to show the existence of a stochastic interpolant whose PDF solves (4.2):

Lemma 4.2. *If Assumption (4.1) holds, then the solution $\rho(t)$ to (4.2) is the PDF of the stochastic interpolant*

$$x_t = T(t, \alpha(t)T^{-1}(0, x_0) + \beta(t)T^{-1}(1, x_1)) + \gamma(t)z, \quad (4.4)$$

as long as $\alpha^2(t) + \beta^2(t) + \gamma^2(t) = 1$.

This lemma is proven in Appendix B.6: (4.4) corresponds to choosing $I(t, x_0, x_1) = T(t, \alpha(t)T^{-1}(t, x_0) + \beta(t)T^{-1}(t, x_1))$ in (2.1). With the help of Lemma 4.2, we can establish the following result showing how to optimize over the function I to solve the Schrödinger bridge problem:

Theorem 4.3. *Pick some $\gamma : [0, 1] \rightarrow [0, 1]$ such that $\gamma(0) = \gamma(1) = 0$, $\gamma(t) > 0$ for $t \in (0, 1)$, $\gamma \in C^2((0, 1))$ and $\gamma^2 \in C^1([0, 1])$, and let $\hat{x}_t = \hat{I}(t, x_0, x_1) + \gamma(t)z$, with $x_0 \sim \rho_0$, $x_1 \sim \rho_1$, $z \sim \mathbf{N}(0, Id)$, all independent. Consider the max-min problem over $\hat{I} \in C^1([0, 1], (C^1(\mathbb{R}^d \times \mathbb{R}^d))^d)$ and $\hat{u} \in C^0([0, 1], (C^1(\mathbb{R}^d))^d)$:*

$$\max_{\hat{I}} \min_{\hat{u}} \int_0^1 \mathbb{E} \left(\frac{1}{2} |\hat{u}(t, \hat{x}_t)|^2 - \left(\partial_t \hat{I}(t, x_0, x_1) + (\dot{\gamma}(t) - \epsilon \gamma^{-1}(t))z \right) \cdot \hat{u}(t, \hat{x}_t) \right) dt, \quad (4.5)$$

If Assumption 4.1 holds, then all the optimizers (I, u) of (4.5) are such that: the PDF of the associated $x_t = I(t, x_0, x_1) + \gamma(t)z$ is the solution ρ to (4.2); and $u = \nabla \lambda$, with λ solution to (4.2).

This theorem is also proven in Appendix B.6. Note that if we fix \hat{I} , the velocity u minimizing this objective is the forward drift b_F defined in (2.17). Note also that if we set $\epsilon \rightarrow 0$, this minimizing velocity field is the velocity field b defined in (2.9), and the max-min problem formally reduces to solving the optimal transport problem: in this case however Assumption 4.1 becomes more stringent as we need to assume that (4.2) with $\epsilon = 0$ (i.e. in the absence of the diffusive terms) have a classical solution. Theorem (4.3) gives us a practical route towards solving the Schrödinger bridge problem with stochastic interpolant. We will leave the numerical investigation of this formulation to future work.

References

- [1] Michael Samuel Albergo and Eric Vanden-Eijnden. Building normalizing flows with stochastic interpolants. In *International Conference on Learning Representations*, 2023.
- [2] D. Bakry and M. Émery. Diffusions hypercontractives. In Jacques Azéma and Marc Yor, editors, *Séminaire de Probabilités XIX 1983/84*, pages 177–206, Berlin, Heidelberg, 1985. Springer Berlin Heidelberg.
- [3] Heli Ben-Hamu, Samuel Cohen, Joey Bose, Brandon Amos, Maximilian Nickel, Aditya Grover, Ricky T. Q. Chen, and Yaron Lipman. Matching normalizing flows and probability paths on manifolds. In Kamalika Chaudhuri, Stefanie Jegelka, Le Song, Csaba Szepesvári, Gang Niu, and Sivan Sabato, editors, *International Conference on Machine Learning, ICML 2022, 17-23 July 2022, Baltimore, Maryland, USA*, volume 162 of *Proceedings of Machine Learning Research*, pages 1749–1763. PMLR, 2022.
- [4] Nicholas M. Boffi and Eric Vanden-Eijnden. Probability flow solution of the fokker-planck equation, 2022.
- [5] Valentin De Bortoli, James Thornton, Jeremy Heng, and Arnaud Doucet. Diffusion schrödinger bridge with applications to score-based generative modeling. In A. Beygelzimer, Y. Dauphin, P. Liang, and J. Wortman Vaughan, editors, *Advances in Neural Information Processing Systems*, 2021.
- [6] Hongrui Chen, Holden Lee, and Jianfeng Lu. Improved analysis of score-based generative modeling: User-friendly bounds under minimal smoothness assumptions. *arxiv:2211.01916*, 2022.

- [7] Ricky T. Q. Chen, Yulia Rubanova, Jesse Bettencourt, and David K Duvenaud. Neural ordinary differential equations. In S. Bengio, H. Wallach, H. Larochelle, K. Grauman, N. Cesa-Bianchi, and R. Garnett, editors, *Advances in Neural Information Processing Systems*, volume 31. Curran Associates, Inc., 2018.
- [8] Scott Chen and Ramesh Gopinath. Gaussianization. In T. Leen, T. Dietterich, and V. Tresp, editors, *Advances in Neural Information Processing Systems*, volume 13. MIT Press, 2000.
- [9] Sitan Chen, Sinho Chewi, Jerry Li, Yuanzhi Li, Adil Salim, and Anru R. Zhang. Sampling is as easy as learning the score: theory for diffusion models with minimal data assumptions. *arXiv:2209.11215*, 2022.
- [10] Yongxin Chen, Tryphon T. Georgiou, and Michele Pavon. Stochastic control liaisons: Richard sinkhorn meets gaspard monge on a schrödinger bridge. *SIAM Review*, 63(2):249–313, 2021.
- [11] Laurent Dinh, Jascha Sohl-Dickstein, and Samy Bengio. Density estimation using real NVP. In *International Conference on Learning Representations*, 2017.
- [12] Tim Dockhorn, Arash Vahdat, and Karsten Kreis. Score-based generative modeling with critically-damped langevin diffusion. In *International Conference on Learning Representations (ICLR)*, 2022.
- [13] Conor Durkan, Artur Bekasov, Iain Murray, and George Papamakarios. Neural spline flows. In H. Wallach, H. Larochelle, A. Beygelzimer, F. d'Alché-Buc, E. Fox, and R. Garnett, editors, *Advances in Neural Information Processing Systems*, volume 32. Curran Associates, Inc., 2019.
- [14] Chris Finlay, Joern-Henrik Jacobsen, Levon Nurbekyan, and Adam Oberman. How to train your neural ODE: the world of Jacobian and kinetic regularization. In Hal Daumé III and Aarti Singh, editors, *Proceedings of the 37th International Conference on Machine Learning*, volume 119 of *Proceedings of Machine Learning Research*, pages 3154–3164. PMLR, 13–18 Jul 2020.
- [15] Jerome H. Friedman. Exploratory projection pursuit. *Journal of the American Statistical Association*, 82(397):249–266, 1987.
- [16] Will Grathwohl, Ricky T. Q. Chen, Jesse Bettencourt, and David Duvenaud. Scalable reversible generative models with free-form continuous dynamics. In *International Conference on Learning Representations*, 2019.
- [17] Jonathan Ho, Ajay Jain, and Pieter Abbeel. Denoising diffusion probabilistic models. In H. Larochelle, M. Ranzato, R. Hadsell, M.F. Balcan, and H. Lin, editors, *Advances in Neural Information Processing Systems*, volume 33, pages 6840–6851. Curran Associates, Inc., 2020.
- [18] Emiel Hoogeboom, Jonathan Heek, and Tim Salimans. simple diffusion: End-to-end diffusion for high resolution images. *arXiv preprint arXiv:2301.11093*, 2023.
- [19] Chin-Wei Huang, Ricky T. Q. Chen, Christos Tsirigotis, and Aaron Courville. Convex potential flows: Universal probability distributions with optimal transport and convex optimization. In *International Conference on Learning Representations*, 2021.
- [20] Chin-Wei Huang, David Krueger, Alexandre Lacoste, and Aaron Courville. Neural autoregressive flows. In Jennifer Dy and Andreas Krause, editors, *Proceedings of the 35th International Conference on Machine Learning*, volume 80 of *Proceedings of Machine Learning Research*, pages 2078–2087. PMLR, 10–15 Jul 2018.
- [21] Aapo Hyvärinen. Estimation of non-normalized statistical models by score matching. *Journal of Machine Learning Research*, 6(24):695–709, 2005.

- [22] Tero Karras, Miika Aittala, Timo Aila, and Samuli Laine. Elucidating the design space of diffusion-based generative models. In *Proc. NeurIPS*, 2022.
- [23] Young-Heon Kim and Emanuel Milman. A generalization of caffarelli’s contraction theorem via (reverse) heat flow. *Mathematische Annalen*, 354:827–862, 2010.
- [24] Diederik P Kingma, Tim Salimans, Ben Poole, and Jonathan Ho. On density estimation with diffusion models. In A. Beygelzimer, Y. Dauphin, P. Liang, and J. Wortman Vaughan, editors, *Advances in Neural Information Processing Systems*, 2021.
- [25] Holden Lee, Jianfeng Lu, and Yixin Tan. Convergence for score-based generative modeling with polynomial complexity. *arXiv:2206.06227*, 2022.
- [26] Holden Lee, Jianfeng Lu, and Yixin Tan. Convergence of score-based generative modeling for general data distributions. In Shipra Agrawal and Francesco Orabona, editors, *Proceedings of The 34th International Conference on Algorithmic Learning Theory*, volume 201 of *Proceedings of Machine Learning Research*, pages 946–985, 2023.
- [27] Christian Léonard. A survey of the schrödinger problem and some of its connections with optimal transport. *Discrete and Continuous Dynamical Systems*, 34(4):1533–1574, 2014.
- [28] Yaron Lipman, Ricky T. Q. Chen, Heli Ben-Hamu, Maximilian Nickel, and Matthew Le. Flow matching for generative modeling. In *The Eleventh International Conference on Learning Representations*, 2023.
- [29] Qiang Liu. Rectified flow: A marginal preserving approach to optimal transport, 2022.
- [30] Xingchao Liu, Chengyue Gong, and Qiang Liu. Flow straight and fast: Learning to generate and transfer data with rectified flow. In *The Eleventh International Conference on Learning Representations*, 2023.
- [31] Cheng Lu, Kaiwen Zheng, Fan Bao, Jianfei Chen, Chongxuan Li, and Jun Zhu. Maximum likelihood training for score-based diffusion ODEs by high order denoising score matching. In Kamalika Chaudhuri, Stefanie Jegelka, Le Song, Csaba Szepesvari, Gang Niu, and Sivan Sabato, editors, *Proceedings of the 39th International Conference on Machine Learning*, volume 162 of *Proceedings of Machine Learning Research*, pages 14429–14460. PMLR, 17–23 Jul 2022.
- [32] Dimitra Maoutsa, Sebastian Reich, and Manfred Opper. Interacting particle solutions of fokker–planck equations through gradient–log–density estimation. *Entropy*, 22(8), 2020.
- [33] Vinod Nair and Geoffrey E. Hinton. Rectified linear units improve restricted boltzmann machines. In *Proceedings of the 27th International Conference on International Conference on Machine Learning*, ICML’10, page 807–814, Madison, WI, USA, 2010. Omnipress.
- [34] Derek Onken, Samy Wu Fung, Xingjian Li, and Lars Ruthotto. Ot-flow: Fast and accurate continuous normalizing flows via optimal transport. *Proceedings of the AAAI Conference on Artificial Intelligence*, 35(10):9223–9232, May 2021.
- [35] F. Otto and C. Villani. Generalization of an inequality by talagrand and links with the logarithmic sobolev inequality. *Journal of Functional Analysis*, 173(2):361–400, 2000.
- [36] George Papamakarios, Theo Pavlakou, and Iain Murray. Masked autoregressive flow for density estimation. In *Proceedings of the 31st International Conference on Neural Information Processing Systems*, NIPS’17, page 2335–2344, Red Hook, NY, USA, 2017. Curran Associates Inc.

- [37] Stefano Peluchetti. Non-denoising forward-time diffusions, 2022.
- [38] Danilo Rezende and Shakir Mohamed. Variational inference with normalizing flows. In Francis Bach and David Blei, editors, *Proceedings of the 32nd International Conference on Machine Learning*, volume 37 of *Proceedings of Machine Learning Research*, pages 1530–1538, Lille, France, 07–09 Jul 2015. PMLR.
- [39] Jascha Sohl-Dickstein, Eric Weiss, Niru Maheswaranathan, and Surya Ganguli. Deep unsupervised learning using nonequilibrium thermodynamics. In Francis Bach and David Blei, editors, *Proceedings of the 32nd International Conference on Machine Learning*, volume 37 of *Proceedings of Machine Learning Research*, pages 2256–2265, Lille, France, 07–09 Jul 2015. PMLR.
- [40] Yang Song, Conor Durkan, Iain Murray, and Stefano Ermon. Maximum likelihood training of score-based diffusion models. In M. Ranzato, A. Beygelzimer, Y. Dauphin, P.S. Liang, and J. Wortman Vaughan, editors, *Advances in Neural Information Processing Systems*, volume 34, pages 1415–1428. Curran Associates, Inc., 2021.
- [41] Yang Song and Stefano Ermon. Generative modeling by estimating gradients of the data distribution. In H. Wallach, H. Larochelle, A. Beygelzimer, F. d'Alché-Buc, E. Fox, and R. Garnett, editors, *Advances in Neural Information Processing Systems*, volume 32. Curran Associates, Inc., 2019.
- [42] Yang Song, Jascha Sohl-Dickstein, Diederik P Kingma, Abhishek Kumar, Stefano Ermon, and Ben Poole. Score-based generative modeling through stochastic differential equations. In *International Conference on Learning Representations*, 2021.
- [43] Xuan Su, Jiaming Song, Chenlin Meng, and Stefano Ermon. Dual diffusion implicit bridges for image-to-image translation. In *The Eleventh International Conference on Learning Representations*, 2023.
- [44] E. G. Tabak and Cristina V. Turner. A family of nonparametric density estimation algorithms. *Communications on Pure and Applied Mathematics*, 66(2):145–164, 2013.
- [45] Esteban G. Tabak and Eric Vanden-Eijnden. Density estimation by dual ascent of the log-likelihood. *Communications in Mathematical Sciences*, 8(1):217 – 233, 2010.
- [46] Alexander Tong, Jessie Huang, Guy Wolf, David Van Dijk, and Smita Krishnaswamy. TrajectoryNet: A dynamic optimal transport network for modeling cellular dynamics. In Hal Daumé III and Aarti Singh, editors, *Proceedings of the 37th International Conference on Machine Learning*, volume 119 of *Proceedings of Machine Learning Research*, pages 9526–9536. PMLR, 13–18 Jul 2020.
- [47] Cédric Villani. *Optimal transport: old and new*, volume 338. Springer, 2009.
- [48] Pascal Vincent. A Connection Between Score Matching and Denoising Autoencoders. *Neural Computation*, 23(7):1661–1674, 2011.
- [49] Zhisheng Xiao, Karsten Kreis, and Arash Vahdat. Tackling the generative learning trilemma with denoising diffusion GANs. In *International Conference on Learning Representations*, 2022.
- [50] Liu Yang and George Em Karniadakis. Potential flow generator with l2 optimal transport regularity for generative models. *IEEE Transactions on Neural Networks and Learning Systems*, 33(2):528–538, 2022.
- [51] Linfeng Zhang, Weinan E, and Lei Wang. Monge-ampère flow for generative modeling, 2018.

A Bridging two Gaussian mixture densities

In this appendix, we consider the case where ρ_0 and ρ_1 are both Gaussian mixture densities. We denote by

$$\begin{aligned} \mathbf{N}(x, |m, C) &= (2\pi)^{-d/2} [\det C]^{-1/2} \exp\left(-\frac{1}{2}(x-m)^\top C^{-1}(x-m)\right), \\ &= (2\pi)^{-d} \int_{\mathbb{R}^d} e^{ik \cdot (x-m) - \frac{1}{2}k^\top C k} dk, \end{aligned} \quad (\text{A.1})$$

the Gaussian probability density with mean vector $m \in \mathbb{R}^d$ and positive-definite symmetric covariance matrix $C = C^\top \in \mathbb{R}^{d \times d}$. We assume that

$$\rho_0(x) = \sum_{i=1}^{N_0} p_i^0 \mathbf{N}(x, |m_i^0, C_i^0), \quad \rho_1(x) = \sum_{i=1}^{N_1} p_i^1 \mathbf{N}(x, |m_i^1, C_i^1) \quad (\text{A.2})$$

where $N_0, N_1 \in \mathbb{N}$, $p_i^0 > 0$ with $\sum_{i=1}^{N_0} p_i^0 = 1$, $m_i^0 \in \mathbb{R}^d$, $C_i^0 = (C_i^0)^\top \in \mathbb{R}^{d \times d}$, positive-definite, and similarly for p_i^1 , m_i^1 , and C_i^1 . We have:

Proposition A.1. *Consider the process x_t defined in (2.1) using the probability densities in (A.2) and the interpolant in (3.1), i.e.*

$$I(t, x_0, x_1) = \alpha(t)x_0 + \beta(t)x_1 \quad (\text{3.1})$$

with $\alpha(t)$ and $\beta(t)$ satisfying (3.2). Denote

$$m_{ij}(t) = \alpha(t)m_i^0 + \beta(t)m_j^1, \quad C_{ij}(t) = \alpha^2(t)C_i^0 + \beta^2(t)C_j^1 + \gamma^2(t)Id, \quad (\text{A.3})$$

where $i = 1, \dots, N_0$, $j = 1, \dots, N_1$. Then the probability density ρ of x_t is the Gaussian mixture density

$$\rho(t, x) = \sum_{i=1}^{N_0} \sum_{j=1}^{N_1} p_i^0 p_j^1 \mathbf{N}(x, |m_{ij}(t), C_{ij}(t)) \quad (\text{A.4})$$

and the velocity b and the score s defined in (2.9) and (2.13) are

$$b(t, x) = \frac{\sum_{i=1}^{N_0} \sum_{j=1}^{N_1} p_i^0 p_j^1 \left(\dot{m}_{ij}(t) + \frac{1}{2} \dot{C}_{ij}(t) C_{ij}^{-1}(t) (x - m_{ij}(t)) \right) \mathbf{N}(x, |m_{ij}(t), C_{ij}(t))}{\sum_{i=1}^{N_0} \sum_{j=1}^{N_1} p_i^0 p_j^1 \mathbf{N}(x, |m_{ij}(t), C_{ij}(t))}, \quad (\text{A.5})$$

and

$$s(t, x) = - \frac{\sum_{i=1}^{N_0} \sum_{j=1}^{N_1} p_i^0 p_j^1 C_{ij}^{-1}(t) (x - m_{ij}(t)) \mathbf{N}(x, |m_{ij}(t), C_{ij}(t))}{\sum_{i=1}^{N_0} \sum_{j=1}^{N_1} p_i^0 p_j^1 \mathbf{N}(x, |m_{ij}(t), C_{ij}(t))}. \quad (\text{A.6})$$

This proposition implies that b and s grow at most linearly in x , and are approximately linear in regions where the modes of $\rho(t, x)$ remain well-separated. In particular, if ρ_0 and ρ_1 are both Gaussian densities, $\rho_0 = N(m_0, C_0)$ and $\rho_1 = N(m_1, C_1)$, we have

$$b(t, x) = \dot{m}(t) + \frac{1}{2} \dot{C}(t) C^{-1}(t) (x - m(t)), \quad (\text{A.7})$$

and

$$s(t, x) = -C^{-1}(t) (x - m(t)), \quad (\text{A.8})$$

where

$$m(t) = \alpha(t)m_0 + \beta(t)m_1, \quad C(t) = \alpha^2(t)C_0 + \beta^2(t)C_1 + \gamma^2(t)Id. \quad (\text{A.9})$$

Note that the probability flow ODE (2.26) associated with the velocity (A.7) is the linear ODE

$$\frac{d}{dt}X_t = \dot{m}(t) + \frac{1}{2}\dot{C}(t)C^{-1}(t)(X_t - m(t)). \quad (\text{A.10})$$

This equation can only be solved analytically if $\dot{C}(t)$ and $C(t)$ commute (which is the case e.g. if $C_0 = Id$), but it is easy to see that it always guarantees that

$$\mathbb{E}_0 X_t(x_0) = m(t), \quad \mathbb{E}_0 [(X_t(x_0) - m(t))(X_t(x_0) - m(t))^\top] = C(t), \quad (\text{A.11})$$

where $X_t(x_0)$ denotes the solution to (A.10) for the initial condition $X_{t=0}(x_0) = x_0$ and \mathbb{E}_0 denotes expectation over $x_0 \sim \rho_0$. A similar statement is true if we solve (A.10) with final conditions at $t = 1$ drawn from ρ_1 . Similarly, the forward SDE (2.27) associated with the velocity (A.7) and the score (A.8) is the linear SDE

$$dX_t^F = \dot{m}(t)dt + \left(\frac{1}{2}\dot{C}(t) - \epsilon\right)C^{-1}(t)(X_t^F - m(t))dt + \sqrt{2\epsilon}dW_t. \quad (\text{A.12})$$

and its solutions are such that

$$\mathbb{E}_0 \mathbb{E}_F^{x_0} X_t^F = m(t), \quad \mathbb{E}_0 \mathbb{E}_F^{x_0} [(X_t^F - m(t))(X_t^F - m(t))^\top] = C(t), \quad (\text{A.13})$$

where $\mathbb{E}_F^{x_0}$ denotes expectation over the solution of (A.12) conditional on the event $X_{t=0}^F = x_0$ and \mathbb{E}_0 denotes expectation over $x_0 \sim \rho_0$. A similar statement also holds for the backward SDE (2.28).

Proof. The characteristic function of $\rho(t, x)$ is given by

$$g(t, k) = \mathbb{E} e^{ik \cdot x_t} = \sum_{i=1}^{N_0} \sum_{j=1}^{N_1} p_i^0 p_j^1 e^{ik \cdot m_{ij}(t) - \frac{1}{2}k^\top C_{ij}(t)k}. \quad (\text{A.14})$$

whose inverse Fourier transform is (A.4). This automatically implies (A.6) since we know from 2.13 that $s = \nabla \log \rho$. To derive (A.7) use the function m defined in (B.12):

$$m(t, k) = \sum_{i=1}^{N_0} \sum_{j=1}^{N_1} p_i^0 p_j^1 \left(\dot{m}_{ij}(t) + \frac{1}{2}i\dot{C}_{ij}(t)k \right) e^{ik \cdot m_{ij}(t) - \frac{1}{2}k^\top C_{ij}^\gamma(t)k}. \quad (\text{A.15})$$

From (B.13), we know that the inverse Fourier transform of this function is $b\rho$, so that we obtain

$$b(t, x)\rho(t, x) = \sum_{i=1}^{N_0} \sum_{j=1}^{N_1} p_i^0 p_j^1 \left(\dot{m}_{ij}(t) + \frac{1}{2}i\dot{C}_{ij}(t)C_{ij}^{-1}(t)(x - m_{ij}(t)) \right) \mathbf{N}(x, |m_{ij}(t), C_{ij}^\epsilon(t)). \quad (\text{A.16})$$

This gives (A.5). □

B Proofs

In this appendix, we provide the details for proofs omitted from the main text. For ease of reading, a copy of the original theorem statement is provided with the proof.

B.1 Proof of Theorems 2.6, 2.7, and 2.8, and Corollary 2.9.

Theorem 2.6 (Stochastic interpolant properties). *The probability distribution of the stochastic interpolant x_t defined in (2.1) is absolutely continuous with respect to the Lebesgue measure at all times $t \in [0, 1]$ and has a time-dependent probability density function (PDF) $\rho(t)$ that satisfies*

$\rho(0) = \rho_0$, $\rho(1) = \rho_1$, $\rho \in C^1([0, 1]; C^p(\mathbb{R}^d))$ for any $p \in \mathbb{N}$, and $\rho(t, x) > 0$ for all $(t, x) \in [0, 1] \times \mathbb{R}^d$. In addition, ρ solves the transport equation

$$\partial_t \rho + \nabla \cdot (b\rho) = 0, \quad (2.8)$$

where we defined the velocity

$$b(t, x) = \mathbb{E}(\partial_t I(t, x_0, x_1) + \dot{\gamma}(t)z | x_t = x). \quad (2.9)$$

This velocity is in $C^0([0, 1]; (C^p(\mathbb{R}^d))^d)$ for any $p \in \mathbb{N}$, and such that

$$\forall t \in [0, 1] \quad : \quad \int_{\mathbb{R}^d} |b(t, x)|^2 \rho(t, x) dx < \infty. \quad (2.10)$$

Proof. Let $g(t, k) = \mathbb{E}e^{ik \cdot x_t}$, $k \in \mathbb{R}^d$, be the characteristic function of $\rho(t, x)$. By the definition of x_t in (2.1),

$$g(t, k) = \mathbb{E}e^{ik \cdot (I(t, x_0, x_1) + \gamma(t)z)}. \quad (B.1)$$

Using the independence between x_0 , x_1 , and z , we have

$$g(t, k) = \mathbb{E}\left(e^{ik \cdot I(t, x_0, x_1)}\right) \mathbb{E}\left(e^{i\gamma(t)k \cdot z}\right) \equiv g_0(t, k)e^{-\frac{1}{2}\gamma^2(t)|k|^2} \quad (B.2)$$

where we defined

$$g_0(t, k) = \mathbb{E}\left(e^{ik \cdot I(t, x_0, x_1)}\right) \quad (B.3)$$

The function $g_0(t, k)$ is the characteristic function of $I(t, x_0, x_1)$ with $x_0 \sim \rho_0$ and $x_1 \sim \rho_1$. From (B.2), we have

$$|g(t, k)| = |g_0(t, k)|e^{-\frac{1}{2}\gamma^2(t)|k|^2} \leq e^{-\frac{1}{2}\gamma^2(t)|k|^2} \quad (B.4)$$

Since $\gamma(t) > 0$ for all $t \in (0, 1)$ by assumption, this shows that

$$\forall p \in \mathbb{N} \quad \text{and} \quad t \in (0, 1) \quad : \quad \int_{\mathbb{R}^d} |k|^p |g(t, k)| dk < \infty \quad (B.5)$$

implying that $\rho(t, \cdot)$ is in $C^p(\mathbb{R}^d)$ for any $p \in \mathbb{N}$ and all $t \in (0, 1)$. From (B.2), we also have

$$\begin{aligned} |\partial_t g(t, k)|^2 &= \left| \mathbb{E}[(ik \cdot \partial_t I_t(x_0, x_1) - \gamma(t)\dot{\gamma}(t)|k|^2)e^{ik \cdot I_t(x_0, x_1)}] \right|^2 e^{-\gamma^2(t)|k|^2} \\ &\leq 2(|k|^2 \mathbb{E}[|\partial_t I_t(x_0, x_1)|^2] + |\gamma(t)\dot{\gamma}(t)|^2 |k|^4) e^{-\gamma^2(t)|k|^2} \\ &\leq 2(|k|^2 M_1 + 4|\gamma(t)\dot{\gamma}(t)|^2 |k|^4) e^{-\gamma^2(t)|k|^2} \end{aligned} \quad (B.6)$$

and

$$\begin{aligned} |\partial_t^2 g(t, k)|^2 &\leq 4(|k|^2 \mathbb{E}[|\partial_t^2 I_t(x_0, x_1)|^2] + (|\dot{\gamma}(t)|^2 + \gamma(t)\ddot{\gamma}(t))^2 |k|^4) e^{-\gamma^2(t)|k|^2} \\ &\quad + 8(|k|^2 \mathbb{E}[|\partial_t^2 I_t(x_0, x_1)|^4] + (\gamma(t)\dot{\gamma}(t))^4 |k|^8) e^{-\gamma^2(t)|k|^2} \\ &\leq 4(|k|^2 M_2 + (|\dot{\gamma}(t)|^2 + \gamma(t)\ddot{\gamma}(t))^2 |k|^4) e^{-\gamma^2(t)|k|^2} \\ &\quad + 8(|k|^2 M_1 \mathbb{E}[|\partial_t^2 I_t(x_0, x_1)|^4] + (\gamma(t)\dot{\gamma}(t))^4 |k|^8) e^{-\gamma^2(t)|k|^2} \end{aligned} \quad (B.7)$$

where in both cases we used (2.7) in Assumption 2.5 to get the last inequalities. These imply that

$$\forall p \in \mathbb{N} \quad \text{and} \quad t \in (0, 1) \quad : \quad \int_{\mathbb{R}^d} |k|^p |\partial_t g(t, k)| dk < \infty; \quad \int_{\mathbb{R}^d} |k|^p |\partial_t^2 g(t, k)| dk < \infty \quad (B.8)$$

indicating that $\partial_t \rho(t, \cdot)$ and $\partial_t^2 \rho(t, \cdot)$ are in $C^p(\mathbb{R}^d)$ for any $p \in \mathbb{N}$, i.e. $\rho \in C^1((0, 1); C^p(\mathbb{R}^d))$ as claimed. To show that ρ is also positive, denote by $\mu_0(t, dx)$ the unique (by the Fourier inversion theorem) probability measure associated with $g_0(t, k)$, i.e. the measure such that

$$g_0(t, k) = \int_{\mathbb{R}^d} e^{ik \cdot x} \mu_0(t, dx). \quad (\text{B.9})$$

From (B.2) and the convolution theorem it follows that we can express ρ as

$$\rho(t, x) = \int_{\mathbb{R}^d} \frac{e^{-|x-y|^2/(2\gamma^2(t))}}{(2\pi\gamma^2(t))^{d/2}} \mu_0(t, dy), \quad (\text{B.10})$$

This shows that $\rho > 0$ for all $(t, x) \in (0, 1) \times \mathbb{R}^d$. Since $x_{t=0} = x_0$ and $x_{t=1} = x_1$ by definition of the interpolant, we also have $\rho(0) = \rho_0$ and $\rho(1) = \rho_1$, which shows that ρ is also positive and in $C^p(\mathbb{R}^d)$ at $t = 0, 1$ by Assumption 2.5. Note that since $\rho \in C^1((0, 1); C^p(\mathbb{R}^d))$ and is positive, we also immediately deduce that $s = \nabla \log \rho = \nabla \rho / \rho \in C^1((0, 1); (C^p(\mathbb{R}^d))^d)$.

To show that ρ satisfies the TE (2.8), take the time derivative of (B.1) to deduce that

$$\partial_t g(t, k) = ik \cdot m(t, k) \quad (\text{B.11})$$

where $m : [0, 1] \times \mathbb{R}^d \rightarrow \mathbb{C}^d$ is the vector-valued function defined as

$$m(t, k) = \mathbb{E} \left((\partial_t I_t(x_0, x_1) + \dot{\gamma}(t)z) e^{ik \cdot x_t} \right). \quad (\text{B.12})$$

By definition of the conditional expectation, $m(t, k)$ can be expressed as

$$\begin{aligned} m(t, k) &= \int_{\mathbb{R}^d} \mathbb{E} \left((\partial_t I_t(x_0, x_1) + \dot{\gamma}(t)z) e^{ik \cdot x_t} | x_t = x \right) \rho(t, x) dx \\ &= \int_{\mathbb{R}^d} e^{ik \cdot x} \mathbb{E} \left((\partial_t I_t(x_0, x_1) + \dot{\gamma}(t)z) | x_t = x \right) \rho(t, x) dx \\ &= \int_{\mathbb{R}^d} e^{ik \cdot x} b(t, x) \rho(t, x) dx \end{aligned} \quad (\text{B.13})$$

where the last equality follows from the definition of b in (2.9). Inserting (B.13) in (B.11), we deduce that this equation can be written in real space as the TE (2.8).

Let us now investigate the regularity of b . To that end, we go back to m , and use the independence between x_0, x_1 , and z , as well as Gaussian integration by part to deduce that

$$m(t, k) = \mathbb{E} \left((\partial_t I(t, x_0, x_1) - i\gamma(t)\dot{\gamma}(t)k) e^{ik \cdot I(t, x_1, x_0)} \right) e^{-\frac{1}{2}\gamma^2(t)|k|^2}, \quad (\text{B.14})$$

As a result

$$\begin{aligned} |m(t, k)|^2 &= \left| \mathbb{E} \left((\partial_t I(t, x_0, x_1) - i\gamma(t)\dot{\gamma}(t)k) e^{ik \cdot I(t, x_1, x_0)} \right) \right|^2 e^{-\gamma^2(t)|k|^2} \\ &\leq 2 \left(\mathbb{E} [|\partial_t I(t, x_0, x_1)|^2] + |\gamma(t)\dot{\gamma}(t)|^2 |k|^2 \right) e^{-\gamma^2(t)|k|^2} \\ &\leq 2M_1 e^{-\gamma^2(t)|k|^2}, \end{aligned} \quad (\text{B.15})$$

and

$$\begin{aligned} |\partial_t m(t, k)|^2 &\leq 4 \left(\mathbb{E} [|\partial_t^2 I(t, x_0, x_1)|^2] + (\gamma(t)\ddot{\gamma}(t) + \dot{\gamma}^2(t))^2 \right) e^{-\gamma^2(t)|k|^2} \\ &\quad + 8|k|^2 \left(\mathbb{E} [|\partial_t I(t, x_0, x_1)|^4] + (\gamma(t)\dot{\gamma}(t))^4 |k|^4 \right) e^{-\gamma^2(t)|k|^2} \\ &\leq 4 \left(M_1 + (\gamma(t)\ddot{\gamma}(t) + \dot{\gamma}^2(t))^2 \right) e^{-\gamma^2(t)|k|^2} \\ &\quad + 8|k|^2 \left(M_2 + (\gamma(t)\dot{\gamma}(t))^4 |k|^4 \right) e^{-\gamma^2(t)|k|^2}, \end{aligned} \quad (\text{B.16})$$

where in both cases the last inequalities follow from (2.7). Therefore

$$\forall p \in \mathbb{N} \quad \text{and} \quad t \in (0, 1) \quad : \quad \int_{\mathbb{R}^d} |k|^p |m(t, k)| dk < \infty, \quad \int_{\mathbb{R}^d} |k|^p |\partial_t m(t, k)| dk < \infty \quad (\text{B.17})$$

which implies that the inverse Fourier transform of m is a function $j : [0, 1] \times \mathbb{R}^d \rightarrow \mathbb{R}^d$ that is in $(C^p(\mathbb{R}^d))^d$ for any $p \in \mathbb{N}$ and can be expressed as

$$j(t, x) = (2\pi)^{-d} \int_{\mathbb{R}^d} e^{-ik \cdot x} m(t, k) dk = \mathbb{E}(\partial_t I(t, x_0, x_1) + \dot{\gamma}(t)z|x_t = x) \rho(t, x) \equiv b(t, x) \rho_t(x) \quad (\text{B.18})$$

where the last equality follows from the definition of b in (2.9). We deduce that $b \in C^0([0, 1]; (C^p(\mathbb{R}^d))^d)$ for any $p \in \mathbb{N}$ since $j \in C^0([0, 1]; (C^p(\mathbb{R}^d))^d)$ and $\rho \in C^1([0, 1]; C^p(\mathbb{R}^d))$, and $\rho > 0$.

Finally, let us establish (2.10). By (2.7) we have

$$\begin{aligned} \int_{\mathbb{R}^d} |b(t, x)|^2 \rho(t, x) dx &= \int_{\mathbb{R}^d} |\mathbb{E}((\partial_t I(t, x_0, x_1) + \dot{\gamma}(t)z|x_t = x))|^2 \rho(t, x) dx \\ &\leq 2 \int_{\mathbb{R}^d} \mathbb{E}(|\partial_t I(t, x_0, x_1)|^2 + |\dot{\gamma}(t)|^2 |z|^2 |x_t = x|) \rho(t, x) dx \\ &\leq 2 \mathbb{E}[|\partial_t I(t, x_0, x_1)|^2 + |\dot{\gamma}(t)|^2 |z|^2] \\ &< M_1^{1/2} + d|\dot{\gamma}(t)|^2. \end{aligned} \quad (\text{B.19})$$

Therefore this integral is bounded for all $t \in (0, 1)$. To analyze its behavior at the end points, notice that the decomposition (2.22) implies that

$$\begin{aligned} b_0(x) &\equiv \lim_{t \rightarrow 0} b(t, x) = \mathbb{E}_1[\partial_t I(0, x, x_1)] - \lim_{t \rightarrow 0} \dot{\gamma}(t) \gamma(t) s_0(x), \\ b_1(x) &\equiv \lim_{t \rightarrow 1} b(t, x) = \mathbb{E}_0[\partial_t I(0, x_0, x)] - \lim_{t \rightarrow 1} \dot{\gamma}(t) \gamma(t) s_1(x), \end{aligned} \quad (\text{B.20})$$

where $s_0 = \nabla \log \rho_0$, $s_1 = \nabla \log \rho_1$, $\mathbb{E} \mathbb{E}_0$ and $\mathbb{E} \mathbb{E}_1$ denotes expectation over $x_0 \sim \rho_0$ and $x_1 \sim \rho_1$ respectively, and we used the property that $x_{t=0} = x_0$ and $x_{t=1} = x_1$. Since $\lim_{t \rightarrow 0, 1} \dot{\gamma}(t) \gamma(t)$ exist by our assumption that $\gamma^2 \in C^1([0, 1])$, it means that b_0 and b_1 are well defined, and

$$\int_{\mathbb{R}^d} |b_0(x)|^2 \rho_0(x) dx < \infty, \quad \int_{\mathbb{R}^d} |b_1(x)|^2 \rho_1(x) dx < \infty \quad (\text{B.21})$$

by Assumption 2.5. As a result the integral in (B.19) it is also continuous at $t = 0, 1$, and as result it must be integrable on $[0, 1]$ and (2.10) holds. \square

Theorem 2.7 (Objective). *The velocity b defined in (2.9) is the unique minimizer in $C^0([0, 1]; (C^1(\mathbb{R}^d))^d)$ of the quadratic objective*

$$\mathcal{L}_b[\hat{b}] = \int_0^1 \mathbb{E} \left(\frac{1}{2} |\hat{b}(t, x_t)|^2 - (\partial_t I(t, x_0, x_1) + \dot{\gamma}(t)z) \cdot \hat{b}(t, x_t) \right) dt \quad (2.12)$$

where x_t is defined in (2.1) and the expectation \mathbb{E} is taken independently over $x_0 \sim \rho_0$, $x_1 \sim \rho_1$, and $z \sim \mathbf{N}(0, Id)$.

Proof. By definition of ρ , the objective \mathcal{L}_b defined in (2.12) can also be written as

$$\begin{aligned} \mathcal{L}_b[\hat{b}] &= \int_{\mathbb{R}^d} \left(\frac{1}{2} |\hat{b}(t, x)|^2 - \mathbb{E}((\partial_t I(t, x_0, x_1) + \dot{\gamma}(t)z|x_t = x) \cdot \hat{b}(t, x)) \right) \rho(t, x) dx \\ &= \int_{\mathbb{R}^d} \left(\frac{1}{2} |\hat{b}(t, x)|^2 - b(t, x) \cdot \hat{b}(t, x) \right) \rho(t, x) dx \end{aligned} \quad (\text{B.22})$$

where we used the definition of b in (2.9). This quadratic objective is bounded from below since

$$\begin{aligned}\mathcal{L}_b[\hat{b}] &= \frac{1}{2} \int_{\mathbb{R}^d} \left| \hat{b}(t, x) - b(t, x) \right|^2 \rho(t, x) dx - \frac{1}{2} \int_{\mathbb{R}^d} |b(t, x)|^2 \rho(t, x) dx \\ &\geq -\frac{1}{2} \int_{\mathbb{R}^d} |b(t, x)|^2 \rho(t, x) dx > -\infty\end{aligned}\tag{B.23}$$

where the last inequality follows from (2.10). Since ρ_t is positive the minimizer of (B.22) is unique and given by $\hat{b} = b$. \square

Theorem 2.8 (Score). *The score of the probability density ρ specified in Theorem 2.6 is in $C^1([0, 1]; (C^p(\mathbb{R}^d))^d)$ for any $p \in \mathbb{N}$ and given by*

$$s(t, x) = \nabla \log \rho(t, x) = -\gamma^{-1}(t) \mathbb{E}(z | x_t = x) \quad \forall (t, x) \in (0, 1) \times \mathbb{R}^d \tag{2.13}$$

In addition it satisfies

$$\forall t \in [0, 1] \quad : \quad \int_{\mathbb{R}^d} |s(t, x)|^2 \rho(t, x) dx < \infty, \tag{2.14}$$

and is the unique minimizer in $C^1([0, 1]; (C^1(\mathbb{R}^d))^d)$ of the quadratic objective

$$\mathcal{L}_s[\hat{s}] = \int_0^1 \mathbb{E} \left(\frac{1}{2} |\hat{s}(t, x_t)|^2 + \gamma^{-1}(t) z \cdot \hat{s}(t, x_t) \right) dt \tag{2.15}$$

where x_t is defined in (2.1) and the expectation \mathbb{E} is taken independently over $x_0 \sim \rho_0$, $x_1 \sim \rho_1$, and $z \sim \mathbf{N}(0, Id)$

Proof. Since $\rho \in C^1((0, 1); C^p(\mathbb{R}^d))$ and is positive by Theorem 2.6, we already know that $s = \nabla \log \rho = \nabla \rho / \rho \in C^1((0, 1); (C^p(\mathbb{R}^d))^d)$. To establish (2.13), note that, for $t \in (0, 1)$ where $\gamma(t) > 0$, we have (this is Gaussian integration by part)

$$\mathbb{E} \left(z e^{i\gamma(t)k \cdot z} \right) = -\gamma^{-1}(t) (i\partial_k) \mathbb{E} e^{i\gamma(t)k \cdot z} = -\gamma^{-1}(t) (i\partial_k) e^{-\frac{1}{2}\gamma^2(t)|k|^2} = \frac{1}{2} i\gamma(t) k e^{-\frac{1}{2}\gamma^2(t)|k|^2}. \tag{B.24}$$

As a result, using the independence between x_0 , x_1 , and z , we have

$$\mathbb{E} \left(z e^{ik \cdot x_t} \right) = \frac{1}{2} i\gamma(t) k g(t, k) \tag{B.25}$$

where g is the characteristic function of x_t defined in (B.1). Using the properties of the conditional expectation, the left hand-side of this equation can be written as

$$\mathbb{E} \left(z e^{i\gamma(t)k \cdot z} \right) = \int_{\mathbb{R}^d} \mathbb{E} \left(z e^{ik \cdot x_t} | x_t = x \right) \rho(t, x) dx = \int_{\mathbb{R}^d} \mathbb{E} (z | x_t = x) e^{ikx_t} \rho(t, x) dx \tag{B.26}$$

Since the left hand side of (B.25) is the Fourier transform of $-\gamma(t)\nabla \rho(t, x)$, we deduce that

$$\mathbb{E} (z | x_t = x) \rho(t, x) = \gamma(t) \nabla \rho(t, x) = \gamma(t) s(t, x) \rho(t, x). \tag{B.27}$$

Since $\rho(t, x) > 0$, this implies (2.13) for $t \in (0, 1)$ where $\gamma(t) > 0$.

To establish (2.14), notice that

$$\begin{aligned}\int_{\mathbb{R}^d} |s(t, x)|^2 \rho(t, x) dx &= \int_{\mathbb{R}^d} |\mathbb{E} ((\gamma^{-1}(t) z | x_t = x))|^2 \rho(t, x) dx \\ &\leq \int_{\mathbb{R}^d} \gamma^{-2}(t) \mathbb{E} (|z|^2 | x_t = x) \rho(t, x) dx \\ &\leq \gamma^{-2}(t).\end{aligned}\tag{B.28}$$

This means that this integral is bounded for all $t \in (0, 1)$. Since it is also continuous at $t = 0, 1$, with values given by (2.6), it must be integrable on $[0, 1]$ and (2.14) holds.

The objective \mathcal{L}_s defined in (2.15) can also be written as

$$\begin{aligned}\mathcal{L}_s[\hat{s}] &= \int_{\mathbb{R}^d} \left(\frac{1}{2} |\hat{s}(t, x)|^2 + \frac{\epsilon}{t(1-t)} \mathbb{E}(B_t | x_t = x) \cdot \hat{s}(t, x) \right) \rho(t, x) dx \\ &= \int_{\mathbb{R}^d} \left(\frac{1}{2} |\hat{s}(t, x)|^2 - s(t, x) \cdot \hat{s}(t, x) \right) \rho(t, x) dx\end{aligned}\tag{B.29}$$

where we used the definition of s in (2.13). This quadratic objective is bounded from below since

$$\begin{aligned}\mathcal{L}_s[\hat{s}] &= \frac{1}{2} \int_{\mathbb{R}^d} |\hat{s}(t, x) - s(t, x)|^2 \rho(t, x) dx - \frac{1}{2} \int_{\mathbb{R}^d} |s(t, x)|^2 \rho(t, x) dx \\ &\geq -\frac{1}{2} \int_{\mathbb{R}^d} |s(t, x)|^2 \rho(t, x) dx > -\infty\end{aligned}\tag{B.30}$$

where the last inequality follows from (2.14). Since ρ is positive the minimizer of (B.29) is unique and given by $\hat{s} = s$. \square

Corollary 2.9 (Fokker Planck equations). *For any $\epsilon \geq 0$, the probability density ρ specified in Theorem 2.6 satisfies:*

1. *The forward Fokker-Planck equation*

$$\partial_t \rho + \nabla \cdot (b_F \rho) = \epsilon \Delta \rho, \quad \rho(0) = \rho_0,\tag{2.16}$$

where we defined the forward drift

$$b_F(t, x) = b(t, x) + \epsilon s(t, x).\tag{2.17}$$

Equation (2.16) is well-posed when solved forward in time from $t = 0$ to $t = 1$, and its solution for the initial condition $\rho(t = 0) = \rho_0$ satisfies $\rho(t = 1) = \rho_1$.

2. *The backward Fokker-Planck equation*

$$\partial_t \rho + \nabla \cdot (b_B \rho) = -\epsilon \Delta \rho, \quad \rho(1) = \rho_1,\tag{2.18}$$

where we defined the backward drift

$$b_B(t, x) = b(t, x) - \epsilon s(t, x).\tag{2.19}$$

Equation (2.18) is well-posed when solved backward in time from $t = 1$ to $t = 0$, and its solution for the final condition $\rho(1) = \rho_1$ satisfies $\rho(0) = \rho_0$.

Proof. The forward FPE (2.16) and the backward FPE (2.18) are direct consequence of the TE (2.8) and (2.13), since the equality

$$\epsilon \Delta \rho = \epsilon \nabla \cdot (\rho \nabla \log \rho) = \epsilon \nabla \cdot (s \rho)\tag{B.31}$$

can be used to convert between these equations. \square

B.2 Proof of Corollary 2.16

Corollary 2.16 (Generative models). *At any time $t \in [0, 1]$, the law of the stochastic interpolant x_t coincides with the law of the three processes X_t , X_t^F , and X_t^B , respectively defined as:*

1. *The solutions of the ordinary differential equation (ODE) (aka probability flow) associated with the transport equation (2.8)*

$$\frac{d}{dt}X_t = b(t, X_t), \quad (2.26)$$

solved either forward in time from the initial data $X_{t=0} \sim \rho_0$ or backward in time from the final data $X_{t=1} = x_1 \sim \rho_1$.

2. *The solutions of the forward SDE associated with the FPE (2.16)*

$$dX_t^F = b_F(t, X_t^F)dt + \sqrt{2\epsilon}dW_t, \quad (2.27)$$

solved forward in time from the initial data $X_{t=0}^F \sim \rho_0$ independent of W .

3. *The solutions of the backward SDE associated with the backward FPE (2.18)*

$$dX_t^B = b_B(t, X_t^B)dt + \sqrt{2\epsilon}dW_t^B, \quad W_t^B = -W_{1-t}, \quad (2.28)$$

solved backward in time from the final data $X_{t=1}^B \sim \rho_1$ independent of W^B .

Proof. The SDE (2.27) and the ODE (2.26) are the evolution equations for the processes whose PDF solve (2.16) and (2.8). The one equation that requires some explaining in the backward SDE (2.28). This backward SDE be solved backward in time from $t = 1$ to $t = 0$, and by definition its solution is $X_t^B = Z_{1-t}^F$ where Z_t^F solves the forward SDE

$$dZ_t^F = -b_B(1-t, Z_t^F)dt + \sqrt{2\epsilon}dW_t \quad (B.32)$$

to be solved forward in time. To see how to write the backward Itô formula (2.30) note that given any $f \in C^1([0, 1]; C_0^2(\mathbb{R}^d))$, we have

$$\begin{aligned} df(1-t, Z_t^F) &= -\partial_t f(1-t, Z_t^F)dt + \nabla f(1-t, Z_t^F) \cdot dY_t + \epsilon \Delta f(1-t, Z_t^F)dt \\ &= (-b_B(1-t, Z_t^F) \cdot \nabla f(1-t, Z_t^F) + \epsilon \Delta f(1-t, Z_t^F))dt \\ &\quad + \sqrt{2\epsilon} \nabla f(1-t, Z_t^F) \cdot dW_t \end{aligned} \quad (B.33)$$

In integral form, this equation can be written as

$$\begin{aligned} f(1, Z_1^F) &= f(1-t, Z_{1-t}^F) \\ &\quad - \int_{1-t}^1 (\partial_t f(1-s, Z_s^F) + b_B(1-s, Z_s^F) \cdot \nabla f(1-s, Z_s^F) - \epsilon \Delta f(1-s, Z_s^F)) ds \\ &\quad - \sqrt{2\epsilon} \int_{1-t}^1 \nabla f(1-s, Z_s^F) \cdot dW_s. \end{aligned} \quad (B.34)$$

Using $X_t^B = Z_{1-t}^F$ and $W_t^B = -W_{1-t}$ and changing integration variable from s to $1-s$, this is

$$\begin{aligned} f(0, X_0^B) &= f(t, X_t^B) + \int_t^1 (-b_B(s, X_s^B) \cdot \nabla f(s, X_s^B) + \epsilon \Delta f(s, X_s^B)) ds \\ &\quad - \sqrt{2\epsilon} \int_0^t \nabla f(s, X_s^B) \cdot dW_s^B, \end{aligned} \quad (B.35)$$

In differential form, this is equivalent to saying that

$$\begin{aligned} df(t, X_t^{\mathbb{B}}) &= \partial_t f(t, X_t^{\mathbb{B}}) dt + \nabla f(t, X_t^{\mathbb{B}}) \cdot dX_t^{\mathbb{B}} - \epsilon \Delta f(X_t^{\mathbb{B}}) dt \\ &= (\partial_t f(t, X_t^{\mathbb{B}}) + b_{\mathbb{B}}(t, X_t^{\mathbb{B}}) \cdot \nabla f(t, X_t^{\mathbb{B}}) - \epsilon \Delta f(t, X_t^{\mathbb{B}})) dt + \sqrt{2\epsilon} \nabla f(t, X_t^{\mathbb{B}}) \cdot dW_t \end{aligned} \quad (\text{B.36})$$

which is the backward Itô formula (2.30). Similarly, by the Itô isometries we have: for any $g \in C^0([0, 1]; (C_0^0(\mathbb{R}^d))^d)$ and $t \in [0, 1]$

$$\mathbb{E}^x \int_{1-t}^1 g(s, Z_s^{\mathbb{F}}) \cdot dW_s = 0, \quad \mathbb{E}^x \left| \int_{1-t}^1 g(s, Z_s^{\mathbb{F}}) \cdot dW_s \right|^2 = \int_{1-t}^1 \mathbb{E}^x |g(s, Z_s^{\mathbb{F}})|^2 ds. \quad (\text{B.37})$$

Written in terms of $X_t^{\mathbb{B}}$, these are (2.31). □

Derivation of (2.25). For any $t \in [0, 1]$ the score is the minimizer of

$$\begin{aligned} & \int_{\mathbb{R}^d} |\hat{s}(t, x) - \nabla \log \rho(t, x)|^2 \rho(t, x) dx \\ &= \int_{\mathbb{R}^d} (|\hat{s}(t, x)|^2 - 2\hat{s}(t, x) \cdot \nabla \log \rho(t, x) + |\nabla \log \rho(t, x)|^2) \rho(t, x) dx \\ &= \int_{\mathbb{R}^d} (|\hat{s}(t, x)|^2 + 2\nabla \cdot \hat{s}(t, x) + |\nabla \log \rho(t, x)|^2) \rho(t, x) dx, \end{aligned} \quad (\text{B.38})$$

where we used the identity $\hat{s} \cdot \nabla \log \rho = \hat{s} \cdot \nabla \rho$ and integration by parts to obtain the second equality. The last term involving $|\nabla \log \rho|^2$ is a constant in \hat{s} that can be neglected for optimization. Expressing the remaining terms as an expectation over x_t and integrating the result in time gives (2.25).

B.3 Proofs of Lemmas 2.19 and 2.20, and Theorem 2.21.

Lemma 2.19. Let $\rho_0 : \mathbb{R}^d \rightarrow \mathbb{R}_{\geq 0}$ denote a fixed base probability density function. Given two velocity fields $b, \hat{b} \in C^0([0, 1], (C^1(\mathbb{R}^d))^d)$, let the time-dependent densities $\rho : [0, 1] \times \mathbb{R}^d \rightarrow \mathbb{R}_{\geq 0}$ and $\hat{\rho} : [0, 1] \times \mathbb{R}^d \rightarrow \mathbb{R}_{\geq 0}$ denote the solutions to the transport equations

$$\begin{aligned} \partial_t \rho + \nabla \cdot (b\rho) &= 0, & \rho(0) &= \rho_0, \\ \partial_t \hat{\rho} + \nabla \cdot (\hat{b}\hat{\rho}) &= 0, & \hat{\rho}(0) &= \rho_0. \end{aligned} \quad (2.32)$$

Then, the Kullback-Leibler divergence of $\rho(1)$ from $\hat{\rho}(1)$ is given by

$$\text{KL}(\rho(1) \parallel \hat{\rho}(1)) = \int_0^1 \int_{\mathbb{R}^d} (\nabla \log \hat{\rho}(t, x) - \nabla \log \rho(t, x)) \cdot (\hat{b}(t, x) - b(t, x)) \rho(t, x) dx dt. \quad (2.33)$$

Proof. Using (2.32), we compute analytically

$$\begin{aligned}
\frac{d}{dt} \text{KL}(\rho(t) \parallel \hat{\rho}(t)) &= \frac{d}{dt} \int_{\mathbb{R}^d} \log \left(\frac{\rho}{\hat{\rho}} \right) \rho dx \\
&= \int_{\mathbb{R}^d} \hat{\rho} \left(\frac{\partial_t \rho}{\hat{\rho}} - \frac{\rho}{(\hat{\rho})^2} \partial_t \hat{\rho} \right) dx + \int \log \left(\frac{\rho}{\hat{\rho}} \right) \partial_t \rho dx \\
&= - \int_{\mathbb{R}^d} \left(\frac{\rho}{\hat{\rho}} \right) \partial_t \hat{\rho} dx + \int_{\mathbb{R}^d} \log \left(\frac{\rho}{\hat{\rho}} \right) \partial_t \rho dx \\
&= \int_{\mathbb{R}^d} \left(\frac{\rho}{\hat{\rho}} \right) \nabla \cdot (\hat{b} \hat{\rho}) dx - \int \log \left(\frac{\rho}{\hat{\rho}} \right) \nabla \cdot (b \rho) dx \\
&= - \int_{\mathbb{R}^d} \nabla \left(\frac{\rho}{\hat{\rho}} \right) \cdot \hat{b} \hat{\rho} dx + \int (\nabla \log \rho - \nabla \log \hat{\rho}) \cdot b \rho dx \\
&= - \int_{\mathbb{R}^d} \left(\frac{\nabla \rho}{\hat{\rho}} - \frac{\rho \nabla \hat{\rho}}{\hat{\rho}^2} \right) \cdot \hat{b} \hat{\rho} dx + \int_{\mathbb{R}^d} (\nabla \log \rho - \nabla \log \hat{\rho}) \cdot b \rho dx \\
&= \int_{\mathbb{R}^d} (\nabla \log \hat{\rho} - \nabla \log \rho) \cdot \hat{b} \rho dx + \int_{\mathbb{R}^d} (\nabla \log \rho - \nabla \log \hat{\rho}) \cdot b \rho dx \\
&= \int_{\mathbb{R}^d} (\nabla \log \hat{\rho} - \nabla \log \rho) \cdot (\hat{b} - b) \rho dx.
\end{aligned}$$

where we omitted the argument (t, x) of all functions for simplicity of notation. Integrating both sides from 0 to 1 completes the proof. \square

Lemma 2.20. Let $\rho_0 : \mathbb{R}^d \rightarrow \mathbb{R}_{\geq 0}$ denote a fixed base probability density function. Given two velocity fields $b_F, \hat{b}_F \in C^0([0, 1], (C^1(\mathbb{R}^d))^d)$, let the time-dependent densities $\rho : [0, 1] \times \mathbb{R}^d \rightarrow \mathbb{R}_{\geq 0}$ and $\hat{\rho} : [0, 1] \times \mathbb{R}^d \rightarrow \mathbb{R}_{\geq 0}$ denote the solutions to the Fokker-Planck equations

$$\begin{aligned}
\partial_t \rho + \nabla \cdot (b_F \rho) &= \epsilon \Delta \rho, & \rho(0) &= \rho_0, \\
\partial_t \hat{\rho} + \nabla \cdot (\hat{b}_F \hat{\rho}) &= \epsilon \Delta \hat{\rho}, & \hat{\rho}(0) &= \rho_0.
\end{aligned} \tag{2.34}$$

Then, the Kullback-Leibler divergence from $\rho(1)$ to $\hat{\rho}(1)$ is given by

$$\begin{aligned}
\text{KL}(\rho(1) \parallel \hat{\rho}(1)) &= \int_0^1 \int_{\mathbb{R}^d} (\nabla \log \hat{\rho}(t, x) - \nabla \log \rho(t, x)) \cdot (\hat{b}_F(t, x) - b_F(t, x)) \rho(t, x) dx dt \\
&\quad - \epsilon \int_0^1 \int_{\mathbb{R}^d} |\nabla \log \rho(t, x) - \nabla \log \hat{\rho}(t, x)|^2 \rho(t, x) dx dt,
\end{aligned} \tag{2.35}$$

and as a result

$$\text{KL}(\rho(1) \parallel \hat{\rho}(1)) \leq \frac{1}{\epsilon} \int_0^1 \int_{\mathbb{R}^d} \left| \hat{b}_F(t, x) - b_F(t, x) \right|^2 \rho(t, x) dx dt. \tag{2.36}$$

Proof. Similar to the proof of Lemma 2.19, we can use the FPE in (2.34) to compute $\frac{d}{dt} \text{KL}(\rho(t) \parallel \hat{\rho}(t))$, which leads to a proof of the main result. Instead, we take a simpler approach, leveraging the result in Lemma 2.19. We re-write the Fokker-Planck equations in (2.34) as the (score-dependent) transport equations

$$\begin{aligned}
\partial_t \rho &= -\nabla \cdot ((b_F - \epsilon \nabla \log \rho) \rho), \\
\partial_t \hat{\rho} &= -\nabla \cdot ((\hat{b}_F - \epsilon \nabla \log \hat{\rho}) \hat{\rho}).
\end{aligned} \tag{B.39}$$

Applying Lemma 2.19 directly, we find that

$$\text{KL}(\rho(1) \parallel \hat{\rho}(1)) = \int_0^1 \int_{\mathbb{R}^d} \left[(\nabla \log \hat{\rho} - \nabla \log \rho) \cdot \left([\hat{b}_F - \epsilon \nabla \log \hat{\rho}] - [b_F - \epsilon \nabla \log \rho] \right) \right] \rho dx dt. \tag{B.40}$$

Expanding the above,

$$\begin{aligned} \text{KL}(\rho(1) \parallel \hat{\rho}(1)) &= \int_0^1 \int_{\mathbb{R}^d} \left[(\nabla \log \hat{\rho} - \nabla \log \rho) \cdot (\hat{b}_{\mathbb{F}} - b_{\mathbb{F}}) \right] \rho dx dt \\ &\quad - \epsilon \int_0^1 \int_{\mathbb{R}^d} \left[|\nabla \log \rho - \nabla \log \hat{\rho}|^2 \right] \rho dx dt, \end{aligned} \quad (\text{B.41})$$

which proves the lemma. \square

Theorem 2.21. *Let ρ denote the solution of the Fokker-Planck equation (2.16). Given two velocity fields $\hat{b}, \hat{s} \in C^0([0, 1], C^1(\mathbb{R}^d, \mathbb{R}^d))$, define*

$$\hat{b}_{\mathbb{F}}(t, x) = \hat{b}(t, x) + \epsilon \hat{s}(t, x), \quad \hat{v}(t, x) = \hat{b}(t, x) + \gamma(t) \dot{\gamma}(t) \hat{s}(t, x) \quad (\text{2.37})$$

where the function γ satisfies the properties listed in Definition 2.1. Let $\hat{\rho}$ denote the solution to the Fokker-Planck equation

$$\partial_t \hat{\rho} + \nabla \cdot (\hat{b}_{\mathbb{F}} \hat{\rho}) = \epsilon \Delta \hat{\rho}, \quad \hat{\rho}(0) = \rho_0. \quad (\text{2.38})$$

Then,

$$\text{KL}(\rho_1 \parallel \hat{\rho}(1)) \leq \frac{1}{2\epsilon} \left(\mathcal{L}_b[\hat{b}] - \min_{\hat{b}} \mathcal{L}_b[\hat{b}] \right) + \frac{\epsilon}{2} \left(\mathcal{L}_s[\hat{s}] - \min_{\hat{s}} \mathcal{L}_s[\hat{s}] \right), \quad (\text{2.39})$$

where $\mathcal{L}_b[\hat{b}]$ and $\mathcal{L}_s[\hat{s}]$ are the objective functions defined in (2.12) and (2.15), and

$$\text{KL}(\rho_1 \parallel \hat{\rho}(1)) \leq \frac{1}{2\epsilon} \left(\mathcal{L}_v[\hat{v}] - \min_{\hat{v}} \mathcal{L}_v[\hat{v}] \right) + \frac{\sup_{t \in [0, 1]} (\gamma(t) \dot{\gamma}(t) + \epsilon)^2}{2\epsilon} \left(\mathcal{L}_s[\hat{s}] - \min_{\hat{v}} \mathcal{L}_s[\hat{s}] \right). \quad (\text{2.40})$$

where $\mathcal{L}_v[\hat{v}]$ is the objective function defined in (2.24).

Proof. Observe that by Proposition 2.16, the target density $\rho_1 = \rho(1, \cdot)$ is the density of the process X_t that evolves according to SDE (2.27). By Lemma 2.20, we then have that

$$\begin{aligned} \text{KL}(\rho_1 \parallel \hat{\rho}(1)) &= \int_0^1 \int_{\mathbb{R}^d} (\nabla \log \hat{\rho} - \nabla \log \rho) \cdot ([\hat{b} + \epsilon \hat{s}] - [b + \epsilon s]) \rho dx dt \\ &\quad - \epsilon \int_0^1 \int_{\mathbb{R}^d} |\nabla \log \rho - \nabla \log \hat{\rho}|^2 \rho_t dx dt. \end{aligned} \quad (\text{B.42})$$

By Young's inequality, it holds for any fixed $\eta > 0$ that

$$\begin{aligned} \text{KL}(\rho_1 \parallel \hat{\rho}(1)) &\leq \int_0^1 \int_{\mathbb{R}^d} \left(\frac{\eta}{2} |\nabla \log \hat{\rho} - \nabla \log \rho|^2 + \frac{1}{2\eta} |\hat{b} - b + \epsilon(s - \hat{s})|^2 \right) \rho dx dt \\ &\quad - \epsilon \int_0^1 \int_{\mathbb{R}^d} |\nabla \log \rho - \nabla \log \hat{\rho}|^2 \rho dx dt, \end{aligned} \quad (\text{B.43})$$

$$\begin{aligned} &= \int_0^1 \frac{1}{2\eta} \int_{\mathbb{R}^d} |\hat{b} - b + \epsilon(s - \hat{s})|^2 \rho_t dx dt \\ &\quad + \left(\frac{1}{2}\eta - \epsilon \right) \int_0^1 \int_{\mathbb{R}^d} |\nabla \log \rho_t - \nabla \log \hat{\rho}_t|^2 \rho_t dx dt. \end{aligned} \quad (\text{B.44})$$

Hence, for $\eta = 2\epsilon$,

$$\text{KL}(\rho_1 \parallel \hat{\rho}(1)) \leq \frac{1}{4\epsilon} \int_0^1 \int_{\mathbb{R}^d} |\hat{b} - b + \epsilon(s - \hat{s})|^2 \rho dx dt. \quad (\text{B.45})$$

Again by Young's inequality, it holds that

$$\text{KL}(\rho_1 \parallel \hat{\rho}(1)) \leq \frac{1}{2\epsilon} \int_0^1 \int_{\mathbb{R}^d} \left(|\hat{b} - b|^2 + \epsilon^2 |s - \hat{s}|^2 \right) \rho_t dx dt. \quad (\text{B.46})$$

Using the definition of $\mathcal{L}_b[\hat{b}]$ and $\mathcal{L}_s[\hat{s}]$ in (2.12), and (2.15), we conclude that

$$\text{KL}(\rho_1 \parallel \hat{\rho}(1)) \leq \frac{1}{2\epsilon} \left(\mathcal{L}_b[\hat{b}] - \min_{\hat{b}} \mathcal{L}_b[\hat{b}] \right) + \frac{\epsilon}{2} \left(\mathcal{L}_s[\hat{s}] - \min_{\hat{s}} \mathcal{L}_s[\hat{s}] \right), \quad (\text{B.47})$$

which is (2.39). Using that $b = v - \gamma\dot{\gamma}s$ and $\hat{b} = \hat{v} - \gamma\dot{\gamma}\hat{s}$, we can write (B.45) as

$$\text{KL}(\rho_1 \parallel \hat{\rho}(1)) \leq \frac{1}{4\epsilon} \int_0^1 \int_{\mathbb{R}^d} |\hat{v} - v - (\gamma(t)\dot{\gamma}(t) + \epsilon)(\hat{s} - s)|^2 \rho dx dt, \quad (\text{B.48})$$

$$\leq \frac{1}{2\epsilon} \int_0^1 \int_{\mathbb{R}^d} \left(|\hat{v} - v|^2 + (\gamma(t)\dot{\gamma}(t) + \epsilon)^2 |\hat{s} - s|^2 \right) \rho dx dt, \quad (\text{B.49})$$

$$\leq \frac{1}{2\epsilon} \left(\mathcal{L}_v[\hat{v}] - \min_{\hat{v}} \mathcal{L}_v[\hat{v}] \right) + \frac{\max_{t \in [0,1]} (\gamma(t)\dot{\gamma}(t) + \epsilon)^2}{2\epsilon} \left(\mathcal{L}_s[\hat{s}] - \min_{\hat{s}} \mathcal{L}_s[\hat{s}] \right). \quad (\text{B.50})$$

□

B.4 Proofs of Lemma 2.23 and Theorem 2.24

Lemma 2.23. *Given the velocity field $\hat{b} \in C^0([0, 1], (C^1(\mathbb{R}^d))^d)$, let $\hat{\rho}$ satisfy the transport equation*

$$\partial_t \hat{\rho} + \nabla \cdot (\hat{b} \hat{\rho}) = 0, \quad (\text{2.44})$$

and let $X_{s,t}(x)$ solve the ODE

$$\frac{d}{dt} X_{s,t}(x) = b(t, X_{s,t}(x)), \quad X_{s,s}(x) = x, \quad t, s \in [0, 1] \quad (\text{2.45})$$

Then, given the PDFs ρ_0 and ρ_1 :

1. The solution to (2.44) for the initial condition $\hat{\rho}(0) = \rho_0$ is given at any time $t \in [0, 1]$ by

$$\hat{\rho}(t, x) = \exp \left(- \int_0^t \nabla \cdot b(\tau, X_{t,\tau}(x)) d\tau \right) \rho_0(X_{t,0}(x)) \quad (\text{2.46})$$

2. The solution to (2.44) for the final condition $\hat{\rho}(1) = \rho_1$ is given at any time $t \in [0, 1]$ by

$$\hat{\rho}(t, x) = \exp \left(\int_t^1 \nabla \cdot b(\tau, X_{t,\tau}(x)) d\tau \right) \rho_1(X_{t,1}(x)) \quad (\text{2.47})$$

Proof. If $\hat{\rho}$ solves the TE (2.44) and $X_{s,t}$ solves the ODE (2.45), we have

$$\begin{aligned} \frac{d}{dt} \hat{\rho}(t, X_{s,t}(x)) &= \partial_t \hat{\rho}(t, X_{s,t}(x)) + b(t, X_{s,t}(x)) \cdot \nabla \hat{\rho}(t, X_{s,t}(x)) \\ &= -\nabla \cdot b(t, X_{s,t}(x)) \hat{\rho}(t, X_{s,t}(x)) \end{aligned} \quad (\text{B.51})$$

This equation implies that

$$\frac{d}{dt} \left(\exp \left(\int_s^t \nabla \cdot b(\tau, X_{s,\tau}(x)) d\tau \right) \hat{\rho}(t, X_{s,t}(x)) \right) = 0. \quad (\text{B.52})$$

Integrating (B.52) on $[0, t]$ and setting $s = t$ in the result gives

$$\hat{\rho}(t, x) = \exp \left(- \int_0^t \nabla \cdot b(\tau, X_{t,\tau}(x)) d\tau \right) \hat{\rho}(0, X_{t,0}(x)) \quad (\text{B.53})$$

If we use the initial condition $\hat{\rho}(0) = \rho_0$, this gives (2.46). Similarly, Integrating (B.52) on $[t, 1]$ and setting $s = t$ in the result gives

$$\hat{\rho}(t, x) = \exp \left(\int_t^1 \nabla \cdot b(\tau, X_{t,\tau}(x)) d\tau \right) \hat{\rho}(1, X_{t,1}(x)) \quad (\text{B.54})$$

If we use the final condition $\hat{\rho}(1) = \rho_1$, this gives (2.47). □

Theorem 2.24. *Given $\epsilon > 0$, and two velocity fields $\hat{b}, \hat{s} \in C^0([0, 1], (C^1(\mathbb{R}^d))^d)$, define*

$$\hat{b}_F(t, x) = \hat{b}(t, x) + \epsilon \hat{s}(t, x), \quad \hat{b}_B(t, x) = \hat{b}(t, x) - \epsilon \hat{s}(t, x), \quad (\text{2.48})$$

and let Y_t^F and Y_t^B be the solution of the following forward and backward SDE:

$$dY_t^F = b_B(t, Y_t^F) dt + \sqrt{2\epsilon} dW_t, \quad (\text{2.49})$$

to be solved forward in time from the initial condition $Y_{t=0}^F = x$ independent of W ; and

$$dY_t^B = b_F(t, Y_t^B) dt + \sqrt{2\epsilon} dW_t^B, \quad W_t^B = -W_{1-t}, \quad (\text{2.50})$$

to be solved backward in time from the final condition $Y_{t=1}^B = x$ independent of W^B . Then, given the PDFs ρ_0 and ρ_1 :

1. The solution to the forward FPE

$$\partial \hat{\rho}_F + \nabla \cdot (\hat{b}_F \hat{\rho}_F) = \epsilon \Delta \hat{\rho}_F, \quad \hat{\rho}_F(0) = \rho_0, \quad (\text{2.51})$$

can be expressed at $t = 1$ as

$$\hat{\rho}_F(1, x) = \mathbb{E}_B^x \left(\exp \left(- \int_0^1 \nabla \cdot \hat{b}_F(t, Y_t^B) dt \right) \rho_0(Y_{t=0}^B) \right), \quad (\text{2.52})$$

where \mathbb{E}_B^x denotes expectation on the path of Y_t^B conditional on $Y_{t=1}^B = x$.

2. The solution to the backward FPE

$$\partial \hat{\rho}_B + \nabla \cdot (\hat{b}_B \hat{\rho}_B) = -\epsilon \Delta \hat{\rho}_B, \quad \hat{\rho}_B(1) = \rho_1, \quad (\text{2.53})$$

can be expressed at any $t = 0$ as

$$\hat{\rho}_B(0, x) = \mathbb{E}_F^x \left(\exp \left(\int_0^1 \nabla \cdot \hat{b}_B(t, Y_t^F) dt \right) \rho_1(Y_{t=1}^F) \right), \quad (\text{2.54})$$

where \mathbb{E}_F^x denotes expectation on the path of Y_t^F conditional on $Y_{t=0}^F = x$.

Proof. Evaluating $d\hat{\rho}_F(t, Y_t^B)$ via the backward Itô formula (2.30) we obtain

$$\begin{aligned} d\hat{\rho}_F(t, Y_t^B) &= \partial_t \hat{\rho}_F(t, Y_t^B) dt + \nabla \hat{\rho}_F(t, Y_t^B) \cdot dY_t^B - \epsilon \Delta \hat{\rho}_F(t, Y_t^B) dt \\ &= \partial_t \hat{\rho}_F(t, Y_t^B) dt + \nabla \hat{\rho}_F(t, Y_t^B) \cdot \hat{b}_F(t, Y_t^B) dt + \sqrt{2\epsilon} \nabla \hat{\rho}_F(t, Y_t^B) \cdot dW_t^B - \epsilon \Delta \hat{\rho}_F(t, Y_t^B) dt \\ &= -\nabla \cdot \hat{b}_F(t, Y_t^B) \hat{\rho}_F(t, Y_t^B) dt + \sqrt{2\epsilon} \nabla \hat{\rho}_F(t, Y_t^B) \cdot dW_t^B. \end{aligned} \quad (\text{B.55})$$

where we used (2.50) in the second step and (2.51) in the last one. This equation can be written as a total differential in the form

$$\begin{aligned} & d \left(\exp \left(- \int_t^1 \nabla \cdot \hat{b}_F(\tau, Y_\tau^B) d\tau \right) \hat{\rho}_F(t, Y_t^B) \right) \\ &= \sqrt{2\epsilon} \exp \left(- \int_t^1 \nabla \cdot \hat{b}_F(\tau, Y_\tau^B) d\tau \right) \nabla \hat{\rho}_F(t, Y_t^B) \cdot dW_t^B, \end{aligned} \quad (\text{B.56})$$

which after integration on $t \in [0, 1]$ becomes

$$\begin{aligned} & \hat{\rho}_F(1, Y_{t=1}^B) - \exp \left(- \int_0^1 \nabla \cdot \hat{b}_F(t, Y_t^B) dt \right) \rho_0(Y_{t=0}^B) \\ &= \sqrt{2\epsilon} \int_0^1 \exp \left(- \int_t^1 \nabla \cdot \hat{b}_F(\tau, Y_\tau^B) d\tau \right) \nabla \hat{\rho}(t, Y_t^B) \cdot dW_t^B. \end{aligned} \quad (\text{B.57})$$

where we used $\hat{\rho}(0) = \rho_0$. Taking an expectation conditioned on the event $Y_{t=1}^B = x$ and using that the term on the right-hand side has mean zero, we find that

$$\hat{\rho}_F(1, Y_{t=1}^B) - \mathbb{E}_B^x \exp \left(- \int_0^1 \nabla \cdot \hat{b}_F(t, Y_t^B) dt \right) \rho_0(Y_{t=0}^B) = 0. \quad (\text{B.58})$$

This gives (2.52).

Similarly, evaluating $d\hat{\rho}(t, Y_t^F)$ via the Itô formula, we obtain

$$\begin{aligned} d\hat{\rho}_B(t, Y_t^F) &= \partial_t \hat{\rho}_B(t, Y_t^F) dt + \nabla \hat{\rho}_B(t, Y_t^F) \cdot dY_t^F + \epsilon \Delta \hat{\rho}_B(t, Y_t^F) dt \\ &= \partial_t \hat{\rho}_B(t, Y_t^F) dt + \nabla \hat{\rho}_B(t, Y_t^F) \cdot \hat{b}_B(t, Y_t^F) dt + \sqrt{2\epsilon} \nabla \hat{\rho}_B(t, Y_t^F) \cdot dW_t + \epsilon \Delta \hat{\rho}_B(t, Y_t^F) dt \\ &= -\nabla \cdot \hat{b}_B(t, Y_t^F) \hat{\rho}_B(t, Y_t^F) dt + \sqrt{2\epsilon} \nabla \hat{\rho}_B(t, Y_t^F) \cdot dW_t. \end{aligned} \quad (\text{B.59})$$

where we used (2.49) in the second step and (2.53) in the last one. This equation can be written as a total differential in the form

$$\begin{aligned} & d \left(\exp \left(\int_0^t \nabla \cdot \hat{b}_B(\tau, Y_\tau^F) d\tau \right) \hat{\rho}_B(t, Y_t^F) \right) \\ &= \sqrt{2\epsilon} \exp \left(\int_0^t \nabla \cdot \hat{b}_B(\tau, Y_\tau^F) d\tau \right) \nabla \hat{\rho}_B(t, Y_t^F) \cdot dW_t. \end{aligned} \quad (\text{B.60})$$

Integrating the above on $t \in [0, 1]$, we find that

$$\begin{aligned} & \exp \left(\int_0^1 \nabla \cdot \hat{b}_B(t, Y_t^F) dt \right) \rho_1(Y_1^F) - \hat{\rho}_B(0, Y_{t=0}^F) \\ &= \sqrt{2\epsilon} \int_0^1 \exp \left(\int_0^t \nabla \cdot \hat{b}_B(\tau, Y_\tau^F) d\tau \right) \nabla \hat{\rho}_B(t, Y_t^F) \cdot dW_t. \end{aligned} \quad (\text{B.61})$$

where we used $\hat{\rho}(1) = \rho_1$. Taking an expectation conditioned on the event $Y_{t=0}^F = x$ and applying the Itô isometry, we deduce that

$$\mathbb{E}_F^x \left(\exp \left(\int_0^1 \nabla \cdot \hat{b}_B(t, Y_t^F) dt \right) \rho_1(Y_{t=1}^F) \right) - \hat{\rho}_B(0, y) = 0. \quad (\text{B.62})$$

This gives (2.54). □

B.5 Proof of Theorem 3.5

Theorem 3.5. *Consider the finite-horizon one-sided stochastic interpolant*

$$y_t = \alpha(t)x_0 + \beta(t)z, \quad (3.24)$$

with x_0 and z drawn independently from ρ_0 and $\mathbf{N}(0, Id)$, respectively, and where the functions α and β^2 are in $C^1([0, 1])$ and satisfy

$$\alpha(0) = \beta(1) = 1; \quad \alpha(1) = \beta(0) = 0; \quad \forall t \in (0, 1) : \alpha(t) > 0, \dot{\alpha}(t) < 0, \beta(t) > 0, \dot{\beta}(t) < 0. \quad (3.25)$$

Then at any time $t \in [0, 1)$, the law of y_t coincides with the law of the solution to the forward SDE

$$dZ_t^F = \alpha^{-1}(t)\dot{\alpha}(t)Z_t^F dt + \sqrt{2D(t)}dW_t, \quad Z_{t=0}^F \sim \rho_0, \quad (3.26)$$

where we defined

$$D(t) = \beta(t)\dot{\beta}(t) - \beta^2(t)\alpha^{-1}(t)\dot{\alpha}(t). \quad (3.27)$$

Proof. For the interpolant y_t defined in (3.24), the velocity b in (3.13) reduces to

$$b(t, x) = \mathbb{E}(\dot{\alpha}(t)x_0 + \dot{\beta}(t)z | y_t = x). \quad (B.63)$$

Since $y_t = \alpha(t)x_0 + \beta(t)z$, this can be written as

$$\begin{aligned} b(t, x) &= \mathbb{E}(\alpha^{-1}(t)\dot{\alpha}(t)y_t + (\dot{\beta}(t) - \beta(t)\alpha^{-1}(t)\dot{\alpha}(t))z | y_t = x) \\ &= \alpha^{-1}(t)\dot{\alpha}(t)x + (\dot{\beta}(t) - \beta(t)\alpha^{-1}(t)\dot{\alpha}(t))\mathbb{E}(z | y_t = x) \\ &= \alpha^{-1}(t)\dot{\alpha}(t)x - D(t)s(t, x) \end{aligned} \quad (B.64)$$

where we used $\mathbb{E}(z | y_t = x) = -\beta(t)s(t, x)$ from (3.14) as well as the definition of $D(t)$ in (3.27). This means that the PDF of y_t satisfies

$$0 = \partial_t \rho + \nabla \cdot ([\alpha^{-1}(t)\dot{\alpha}(t)x - D(t)s(t, x)]\rho(t, x)) = \partial_t \rho + \nabla \cdot (\alpha^{-1}(t)\dot{\alpha}(t)x\rho(t, x)) - D(t)\Delta \rho. \quad (B.65)$$

where we used $s\rho = \nabla \log \rho \rho = \nabla \rho$. The forward SDE associated with this forward FPE is (3.26). \square

B.6 Proof of Lemma 4.2 and Theorem 4.3.

Lemma 4.2. *If Assumption (4.1) holds, then the solution $\rho(t)$ to (4.2) is the PDF of the stochastic interpolant*

$$x_t = T(t, \alpha(t)T^{-1}(0, x_0) + \beta(t)T^{-1}(1, x_1)) + \gamma(t)z, \quad (4.4)$$

as long as $\alpha^2(t) + \beta^2(t) + \gamma^2(t) = 1$.

Proof. By the definition of the map T in (4.3), if $x_0 \sim \rho_0$ and $x_1 \sim \rho_1$, then $T^{-1}(0, x_0) \sim \mathbf{N}(0, Id)$ and $T^{-1}(1, x_1) \sim \mathbf{N}(0, Id)$. As a result, since x_0 , x_1 , and z are independent, and $z \sim \mathbf{N}(0, Id)$, we have

$$\alpha(t)T^{-1}(0, x_0) + \beta(t)T^{-1}(1, x_1) + \gamma(t)z \sim \mathbf{N}(0, \alpha^2(t)Id + \beta^2(t)Id + \gamma^2(t)Id) = \mathbf{N}(0, Id) \quad (B.66)$$

where the second equality follows from the condition $\alpha^2(t) + \beta^2(t) + \gamma^2(t) = 1$. Therefore, using again the definition of the map T

$$T(t, \alpha(t)T^{-1}(0, x_0) + \beta(t)T^{-1}(1, x_1) + \gamma(t)z) \sim \rho(t), \quad (B.67)$$

and we are done. \square

Theorem 4.3. *Pick some $\gamma : [0, 1] \rightarrow [0, 1]$ such that $\gamma(0) = \gamma(1) = 0$, $\gamma(t) > 0$ for $t \in (0, 1)$, $\gamma \in C^2((0, 1))$ and $\gamma^2 \in C^1([0, 1])$, and let $\hat{x}_t = \hat{I}(t, x_0, x_1) + \gamma(t)z$, with $x_0 \sim \rho_0$, $x_1 \sim \rho_1$, $z \sim \mathcal{N}(0, Id)$, all independent. Consider the max-min problem over $\hat{I} \in C^1([0, 1], (C^1(\mathbb{R}^d \times \mathbb{R}^d))^d)$ and $\hat{u} \in C^0([0, 1], (C^1(\mathbb{R}^d))^d)$:*

$$\max_{\hat{I}} \min_{\hat{u}} \int_0^1 \mathbb{E} \left(\frac{1}{2} |\hat{u}(t, \hat{x}_t)|^2 - \left(\partial_t \hat{I}(t, x_0, x_1) + (\dot{\gamma}(t) - \epsilon \gamma^{-1}(t))z \right) \cdot \hat{u}(t, \hat{x}_t) \right) dt, \quad (4.5)$$

If Assumption 4.1 holds, then all the optimizers (I, u) of (4.5) are such that: the PDF of the associated $x_t = I(t, x_0, x_1) + \gamma(t)z$ is the solution ρ to (4.2); and $u = \nabla \lambda$, with λ solution to (4.2).

Proof. Denote by $\hat{\rho}(t, x)$ be the PDF of \hat{x}_t and define the current $\hat{j} : [0, 1] \times \mathbb{R}^d \rightarrow \mathbb{R}^d$ as

$$\hat{j}(t, x) = \mathbb{E}(\partial_t \hat{I}_t + \gamma(t)z | x = \hat{x}_t) \hat{\rho}(t, x) \quad (B.68)$$

In terms of this density and this current, the max-min problem (4.5) can be formulated as the constrained optimization problem:

$$\begin{aligned} \max_{\hat{\rho}, \hat{j}} \min_{\hat{u}} \int_0^1 \int_{\mathbb{R}^d} \left(\frac{1}{2} |\hat{u}(t, x)|^2 \hat{\rho}(t, x) - \hat{u}(t, x) \cdot \hat{j}(t, x) \right) dx dt \\ \text{subject to: } \partial_t \hat{\rho} + \nabla \cdot \hat{j} = \epsilon \Delta \hat{\rho}, \quad \hat{\rho}(t=0) = \rho_0, \quad \hat{\rho}(t=1) = \rho_1 \end{aligned} \quad (B.69)$$

To solve this problem we can use the extended objective

$$\begin{aligned} \max_{\hat{\rho}, \hat{j}} \min_{\hat{u}} \left(\int_0^1 \int_{\mathbb{R}^d} \left(\frac{1}{2} |\hat{u}(t, x)|^2 \hat{\rho}(t, x) - \hat{u}(t, x) \cdot \hat{j}(t, x) \right) dx dt \right. \\ \left. - \int_0^1 \int_{\mathbb{R}^d} \lambda(t, x) (\partial_t \hat{\rho}(t, x) + \nabla \cdot \hat{j}(t, x) - \epsilon \Delta \hat{\rho}(t, x)) dx dt \right. \\ \left. + \int_{\mathbb{R}^d} \eta_0(x) (\hat{\rho}(0, x) - \rho_0(x)) dx - \int_{\mathbb{R}^d} \eta_1(x) (\hat{\rho}(1, x) - \rho_1(x)) dx \right) \end{aligned} \quad (B.70)$$

where $\lambda(t, x)$, $\eta_0(x)$, and $\eta_1(x)$ are Lagrange multipliers used to enforce the constraints. The unique minimizer (ρ, j, λ) of this optimization problem solves the Euler-Lagrange equations:

$$\begin{aligned} \partial_t \rho + \nabla \cdot j &= \epsilon \Delta \rho, \quad \rho(t=0) = \rho_0 \quad \rho(t=1) = \rho_1 \\ \partial_t \lambda + \frac{1}{2} |u|^2 &= -\epsilon \Delta \lambda, \\ j &= u \rho \\ u &= \nabla \lambda \end{aligned} \quad (B.71)$$

We can use the last two equations to write the first two as (4.2), with $u = \nabla \lambda$. Since under Assumption 4.1 that there is an interpolant that realizes the PDF $\rho(t)$ solution to (4.2), we conclude that a optimizer (I, u) of the the max-min problem (4.5) exists, and for any optimizer, I will be such $\rho(t)$ is the PDF of $x_t = I(t, x_0, x_1) + \gamma(t)z$ and $u = \nabla \lambda$. \square

C Experimental Specifications

Details for the experiments regarding learning to sample under the checkerboard density are provided here. Feed forward neural networks of depth 4 and width 512 are used for each model of the velocity b . Training was done for 7000 iterations on batches comprised of 25 draws from the base, 400 draws from the target, and 100 time slices. At each iteration, a variance reduction technique based on antithetic sampling, as in [40]. The objectives given in (2.12) and (2.15) were optimized using the Adam optimizer. The learning rate was set to .002 and was dropped by a factor of 2 every 1500 iterations of training. To integrate the ODE/SDE when drawing samples, we used the Heun-based integrator as suggested in [22].